

---

# Foraminiferal and Palynological Record of an Abrupt Environmental Change at the Badenian/Sarmatian Boundary (Middle Miocene): A Case Study in Northeastern Central Paratethys

---

Danuta Peryt , Przemysław Gedl , [Elżbieta Worobiec](#) , Grzegorz Worobiec , [Tadeusz Marek Peryt](#) \*

Posted Date: 19 January 2024

doi: 10.20944/preprints202401.1471.v1

Keywords: Foraminifers; palynofacies; dinocysts; pollen and spores; Miocene; Central Paratethys; Carpathian Foredeep; Poland



Preprints.org is a free multidiscipline platform providing preprint service that is dedicated to making early versions of research outputs permanently available and citable. Preprints posted at Preprints.org appear in Web of Science, Crossref, Google Scholar, Scilit, Europe PMC.

Copyright: This is an open access article distributed under the Creative Commons Attribution License which permits unrestricted use, distribution, and reproduction in any medium, provided the original work is properly cited.

Article

# Foraminiferal and Palynological Record of an Abrupt Environmental Change at the Badenian/Sarmatian Boundary (Middle Miocene): A Case Study in Northeastern Central Paratethys

Danuta Peryt <sup>1</sup>, Przemysław Gedl <sup>2</sup>, Elżbieta Worobiec <sup>3</sup>, Grzegorz Worobiec <sup>3</sup> and Tadeusz Marek Peryt <sup>4,\*</sup>

<sup>1</sup> Institute of Paleobiology, Polish Academy of Sciences, Twarda 51/55, 00-818 Warszawa, Poland; danuta.peryt@twarda.pan.pl

<sup>2</sup> Institute of Geological Sciences, Polish Academy of Sciences, Research Centre in Kraków, Senacka 1, 31-002 Kraków, Poland; ndgedl@cyf-kr.edu.pl

<sup>3</sup> W. Szafer Institute of Botany, Polish Academy of Sciences, Lubicz 46, 31-512 Kraków, Poland; e.worobiec@botany.pl (E.W.); g.worobiec@botany.pl (G.W.)

<sup>4</sup> Polish Geological Institute – National Research Institute, Rakowiecka 4, 00-975 Warszawa, Poland

\* Correspondence: tadeusz.peryt@pgi.gov.pl

**Abstract:** The Badenian/Sarmatian boundary in the Central Paratethyan basins is characterized by a change from open marine conditions during the late Badenian to the assumed brackish conditions during the early Sarmatian. Foraminiferal and palynological results of the Badenian/Sarmatian boundary interval in the Babczyn 2 borehole (SE Poland) showed that the studied interval accumulated under variable, unstable sedimentary conditions. The Badenian/Sarmatian boundary as correlated with a sudden extinction of stenohaline foraminifera is interpreted as due to the shallowing of the basin. The lack of foraminifera and palynomorphs just above the Badenian/Sarmatian boundary can reflect short-term anoxia. The composition of euryhaline assemblages characteristic for the lower Sarmatian part of the studied succession indicates marine to hypersaline conditions.

**Keywords:** foraminifers; palynofacies; dinocysts; pollen and spores; Miocene; Central Paratethys; Carpathian Foredeep; Poland

## 1. Introduction

The largest faunal turnover event in the Paratethys – a large epicontinental sea extending from Central Europe to inner Asia since the Oligocene [1] – occurred in the Middle Miocene, at the Badenian/Sarmatian boundary, when 94% of the Badenian species became extinct (Badenian–Sarmatian Extinction Event – BSEE; [2]). It was proposed that the cause of this event was a drastic basin-wide change in water chemistry from open marine conditions during the late Badenian to brackish conditions in the Central Paratethyan basins during the early Sarmatian. The details of this transformation are still under discussion, though [3]. [4] concluded that there is no evidence of shallowing associated with the BSEE. [5] suggested that due to a complex tectonic evolution, the closure of the Paratethyan basins at the end of Badenian was most probably diachronous and thus slightly different ages for the Badenian/Sarmatian boundary across the Paratethys should be expected.

This study presents foraminiferal and palynological results of the upper Badenian–Sarmatian strata in one borehole section, namely Babczyn 2, located in the north-eastern part of the Carpathian Foredeep, which is the largest Central Paratethyan Basin (Figure 1). The aim of this study was to identify environmental changes around the inferred Badenian/Sarmatian boundary. The studied borehole is a key section of the northern marginal part of the Carpathian Foredeep [3,6–8]. A recent

biostratigraphic study of two boreholes including Babczyn 2 [8] confirmed, in general, zonation based on foraminifera that was previously established within the Badenian and Sarmatian strata of the northern margin of the Carpathian Foredeep [9-13; cf. 14]. In the upper Badenian, the lower *Neobulimina longa* Zone and the upper *Cibicides crassiseptatus* (*Hanzawaia crassiseptata*) Zone occur; the latter is considered to be synchronous with the *Velapertina* (= *Praeorbulina*) *indigena* (Łuczkowska) planktonic foraminiferal zone [15]. Several foraminiferal zones have been identified in the Sarmatian strata. The lowest foraminiferal zone in the Babczyn 2 borehole was the *Elphidium angulatum* Partial Range Zone occurring below the *Anomalinoides dividens* Interval Zone [8] that is commonly regarded as the lowest Sarmatian (eco)zone (e.g., [11,13,16,17]).

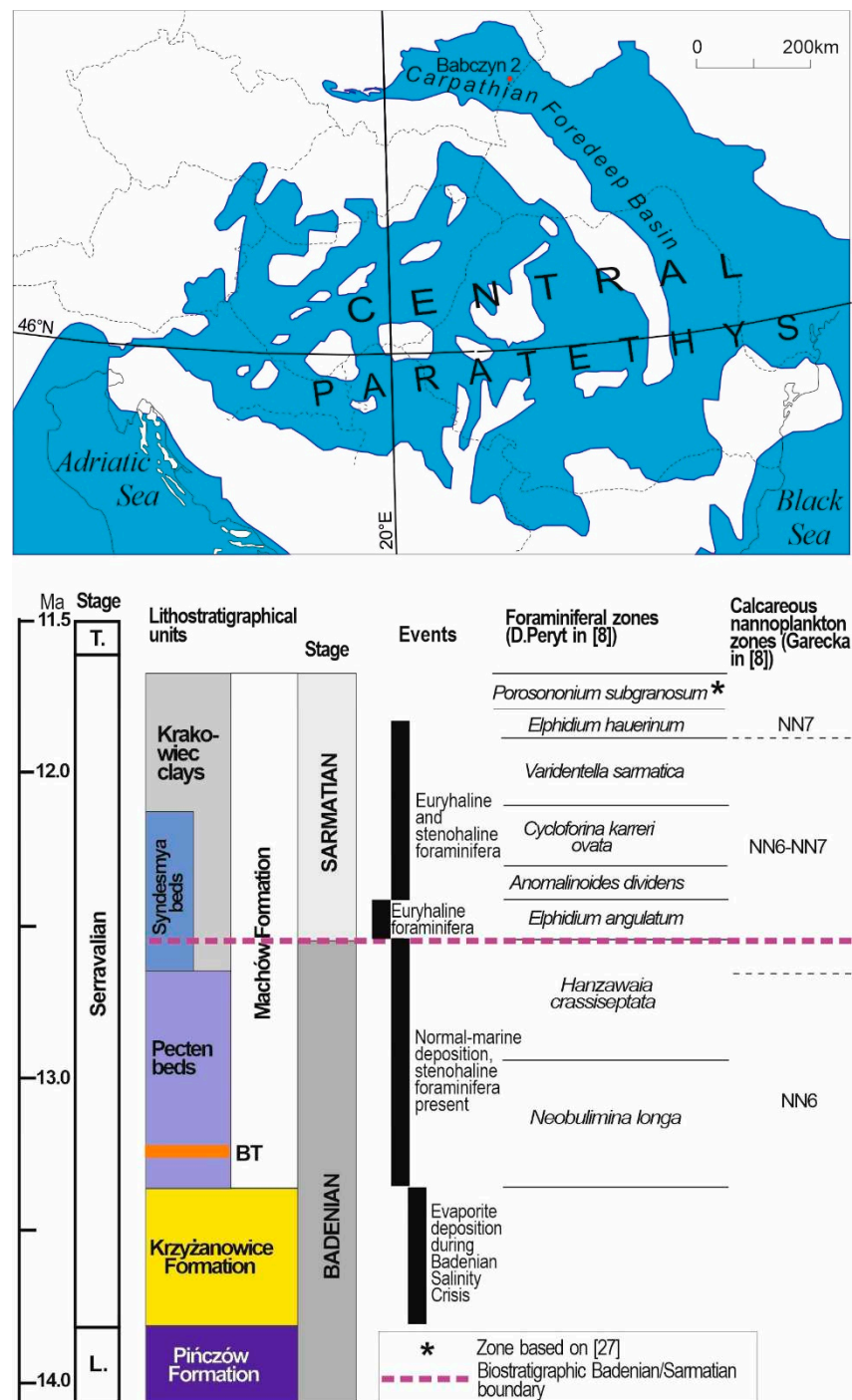


**Figure 1.** Central Paratethys realm in Middle Miocene (modified after [26]) and the location and stratigraphic position of the Babczyn 2 section (modified after [8]); BT – Babczyn Tuff (see [3]); L – Langhian; T. – Tortonian.

The Carpathian Foredeep basin developed in front of the West Carpathians in the Early Miocene and is subdivided into inner and outer parts [18]. The fill is mostly composed of Middle Miocene (Badenian and Sarmatian) deposits. The Badenian and Sarmatian strata in this northern marginal part are several hundred metres thick, and towards the axial part of the Carpathian Foredeep their thickness increases to more than 4 km.

Langhian red-algal limestones and quartz arenites of the Pińczów Formation originated from shelf and near-shore environments, and mudstones and clays originated from more basinal locations (e.g., [19]). Their thickness in the Babczyn 2 borehole is approximately 12 m. These are overlain by Serravalian gypsum of the Krzyżanowice Formation [20] deposited during the Badenian Salinity Crisis ([21], with references therein). The gypsum sequence is 32 m thick [6]. In the uppermost part, an intercalation (2.3 m thick) of marly clays with marine palynomorphs (dinoflagellate cysts) and foraminiferal assemblages occurs [7]. It originated from a short-lived marine transgression to the Badenian evaporite basin, prior to the transgression re-installing normal marine conditions in the Carpathian Foredeep Basin, which resulted from the reconnection of the basin with the Mediterranean and Eastern Paratethys, primarily by tectonic modification of the interconnecting gateways [22].

Consequently, the Serravalian gypsum is overlain by the sandy-silty series of the Machów Formation. Its upper Badenian part is referred to as the Pecten Beds [23]. They are, in turn, overlain by Syndesmya Beds, which were considered to be Sarmatian by [23]. [3] confirmed the location of the Badenian–Sarmatian boundary between the Pecten and Syndesmya Beds at the highest occurrence of well-preserved and identifiable pectinid shells. The location was 6.0 m above the tuff found in the middle portion of the Pecten Beds and 3.4 m above the gypsum, which constrained its depositional age to  $13.06 \pm 0.11$  Ma [3]. This age was calibrated against the same astronomically tuned FCs standard (e.g. [22]), giving the age of  $13.41 \pm 0.10$  Ma, which was comparable to the age of  $13.32 \pm 0.07$  Ma recorded in a volcanic ash layer, located several metres above the Badenian evaporites, in the Romanian East Carpathians [22]. This recalibrated age was used as shown in Figure 1.

The Syndesmya Beds form the lowermost part of the Krakowiec Clays ([24,25], with references therein; Figure 1). [8] proved that the Badenian–Sarmatian boundary lies within the Syndesmya Beds (Figure 1), and not at their base, as previously was assumed. The thickness of the Machów Formation in the Babczyn 2 borehole is almost 400 m; however, only the lowermost part of the formation was cored, and its coring started at a depth of 350 m [23].

## 2. Materials and Methods

A total of 51 samples from the 40.7 m thick interval (368.4–409.1 m depth) in the Babczyn 2 section were studied for foraminifera (samples 8–59); the same sample set was previously [8] used for biostratigraphical study [8]. The sampling distance was ~1 m in the Pecten beds (samples 8–21), 0.5 m in the lowermost part of the Krakowiec clays (samples 22–29) and ~1 m in the higher part of the studied interval of Krakowiec clays (samples 32–59). The most common and characteristic species are illustrated in Figures 2 and 3. The figured specimens were deposited at the Institute of Paleobiology, Polish Academy of Sciences, Warszawa, Poland (ZPAL F. 75).

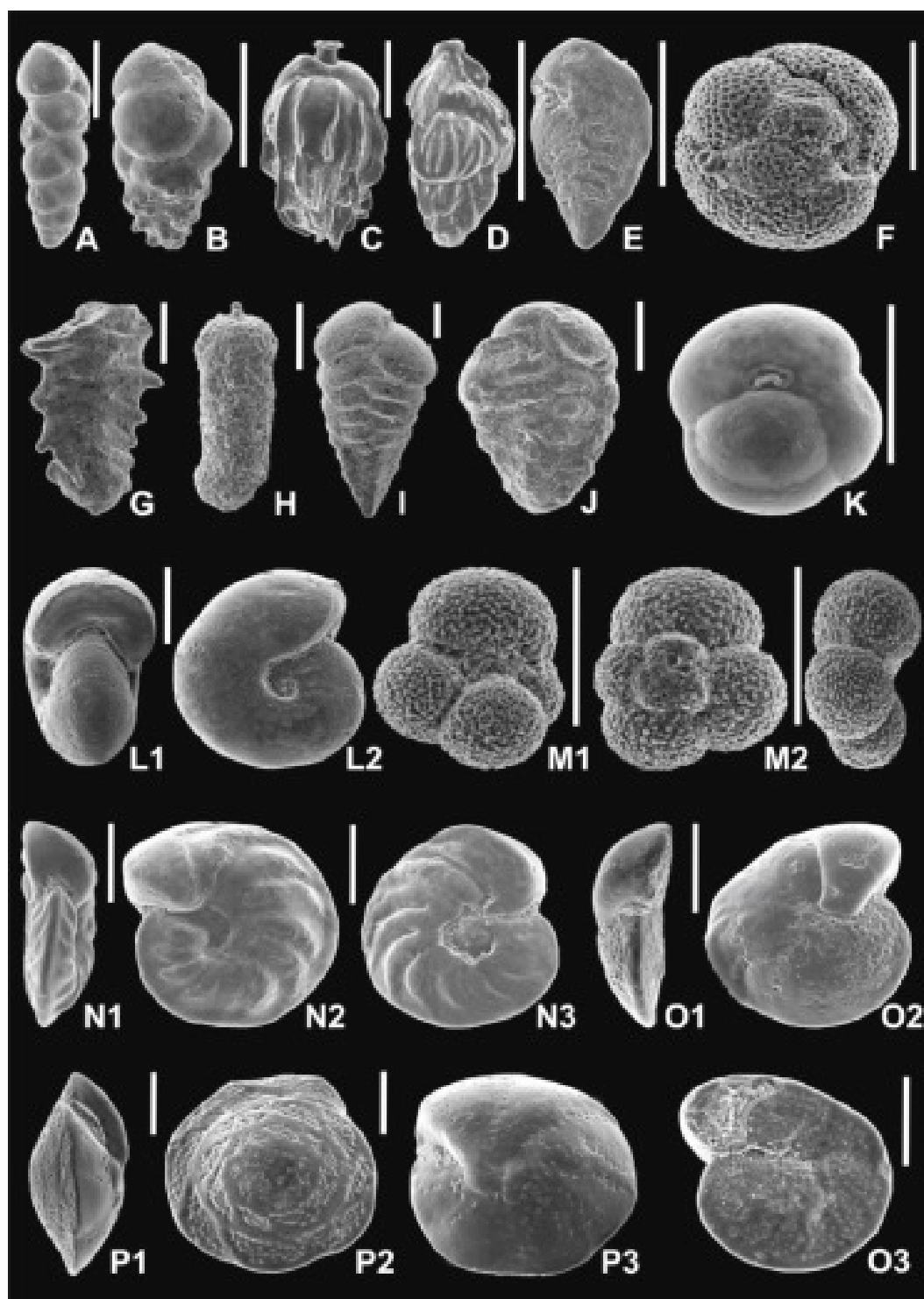


**Figure 2.** Foraminifera from the Babczyn 2 borehole. **A** – *Neobulimina longa* Venglinskyi, sample 17; **B** – *Bulimina subulata* Cushman & Parker, sample 17; **C** – *Uvoigerina bellicostata* Łuczkowska, sample 19; **D** – *Angulogerina angulosa* (Williamson), sample 20; **E** – *Bolivina dilatata* Reuss, sample 17; **F** – *Velapertina indigena* (Łuczkowska), sample 28; **G** – *Spirorutilus carinatus* (d’Orbigny), sample 31; **H** – *Martinottiella communis* (d’Orbigny), sample 28; **I** – *Pseudogaudryina karreriana* (Cushman), sample 25; **J** – *Siphotextularia inopinata* Łuczkowska, sample 28; **K** – *Sphaeroidina bulloides* d’Orbigny, sample 11; **L** – *Melonis pompilioides* (Fichtel & Moll), sample 22; **M** – *Trilobatus* sp., sample 28; **N** – *Hanzawaia crassiseptata* (Łuczkowska), sample 28; **O** – *Lobatula lobatula* (Walker & Jacob), sample 28; **P** – *Heterolepa dutemplei* (d’Orbigny), sample 28; scale bars – 200  $\mu$ m.

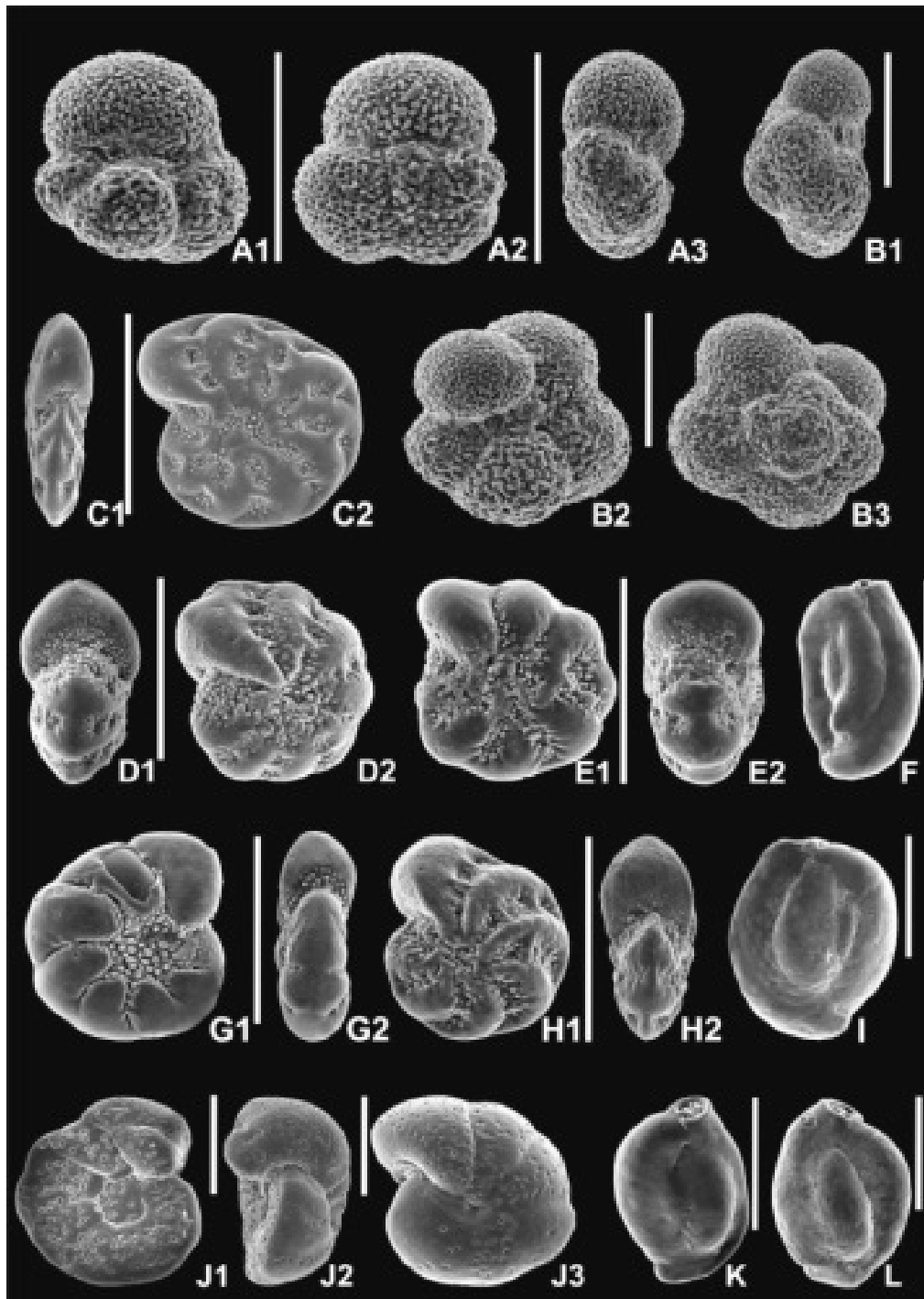


**Figure 3.** Foraminifera from the Babczyn 2 borehole. **A** – *Trilobatus* sp., sample 28; **B** – *Globigerina tarchanensis* Subbotina & Chutzieva, sample 28; **C** – *Elphidium advenum limbatum* (Chapman), sample 33; **D** – *Elphidium angulatum* (Egger), sample 29; **E** – *Elphidiella serena* (Venglinsky), sample 29; **F** – *Quinqueloculina akneriana* d'Orbigny, sample 32; **G** – *Porosonion martkobi* (Bogdanowicz), sample 31; **N** – *Elphidium angulatum* (Egger), sample 29; **P** – *Varidentella reussi* (Bogdanowicz), sample 32; **J** – *Anomalinooides dividens* Łuczkowska, sample 35; **K-L** – *Varidentella reussi* (Bogdanowicz), sample 32; scale bars – 200  $\mu$ m.

Depending on foraminiferal abundances in different samples all foraminifera (up to 200 specimens) were picked. The relative abundances of planktonic and benthic foraminifera within the foraminiferal assemblages (P/B ratio), the Shannon–Weaver heterogeneity index H(S), the relative abundance of the most common genera and the relative abundance of infaunal and epifaunal

morphogroups within the benthic foraminiferal assemblages were calculated (Figure 4). The palaeoenvironmental interpretation based on foraminifera involves the requirements of present-day representatives of recorded taxa [28–39].

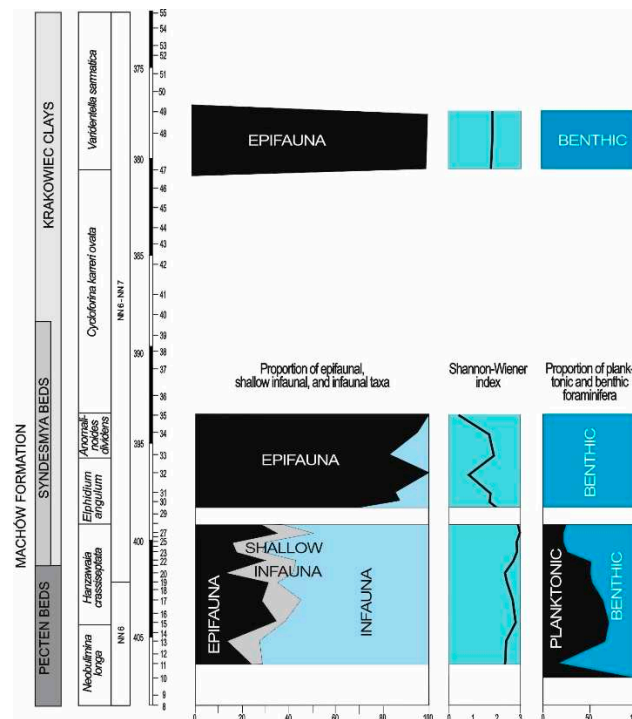


**Figure 4.** The relative abundance (in percent) of epifaunal, shallow infaunal, and infaunal taxa, the Shannon-Wiener index  $H(S)$  and percentage of planktonic foraminifera in foraminiferal assemblages (P/B ratio).

The following taxa were included into the oxic group: *Anomalinoides* spp., *Cibicidoides* spp., *Hansenisca soldanii*, *Hanzawaia* spp., *Heterolepa dutemplei*, *Lobatula lobatula*, *Valvulineria complanata*, *Spirorutilus spcarinatus*, keeled elphidiids, and miliolids. Oxic indices represent epifaunal species. Taxa tolerant of suboxic environments included *Astrononion perfossum*, *Melonis pompilioides* and *Sphaeroidina bulloides*; taxa tolerant of dysoxic environments included *Globocassidulina subglobosa*, *Bolivina* spp., *Bulimina* spp., *Angulogerina*, and *Uvigerina* spp. Foraminifera tolerant of suboxic environments represent mostly shallow infaunal species, whereas foraminifera tolerant of dysoxic environments represent mostly deep infauna and species with opportunistic behaviours. These are commonly used as stress markers (e.g., [40–43]).

For palaeoecological analysis, species or groups of species which at least in one sample exceeded 5 were taken into account. There is a direct relationship between the abundance of species within a community and the environment. Abundance fluctuations of benthic foraminifera are sensitive palaeoceanographic indicators responding to changing palaeotemperature, salinity, nutrient supply and oxygen conditions. Extinction of several rare species would have a minor impact on the total population as their combined species abundances are not likely to exceed 2-10%. Extinction of one or more of the dominant species, however, would have a major impact as they may comprise 50% or more of the total population and reflect a significant environmental change.

For palynology, 26 samples were studied (i.e., the odd sample numbers from 9 to 55 and the even numbers 8 and 28). Applied palynological procedure included 38% hydrochloric acid (HCl) treatment, 40% hydrofluoric acid (HF) treatment, heavy-liquid ( $ZnCl_2+HCl$ ; density  $2.0\text{ g}\cdot\text{cm}^{-3}$ ) separation, ultrasound for 10–15 s and sieving at  $10\ \mu\text{m}$ , on a nylon mesh. No nitric acid ( $HNO_3$ ) treatment was applied. Each processed rock sample weight was 10 g. Two slides from each sample were prepared using glycerine jelly as a mounting medium. The same set of slides was used for the analyses of dinoflagellate cysts, palynofacies (P.G.), and sporomorphs (E.W. and G.W.). Unprocessed

rock samples, palynological residues and slides were stored in the collection of the Institute of Geological Sciences, Polish Academy of Sciences, Research Centre in Kraków, Poland. The most common and characteristic species are illustrated in Figures 5 and 6

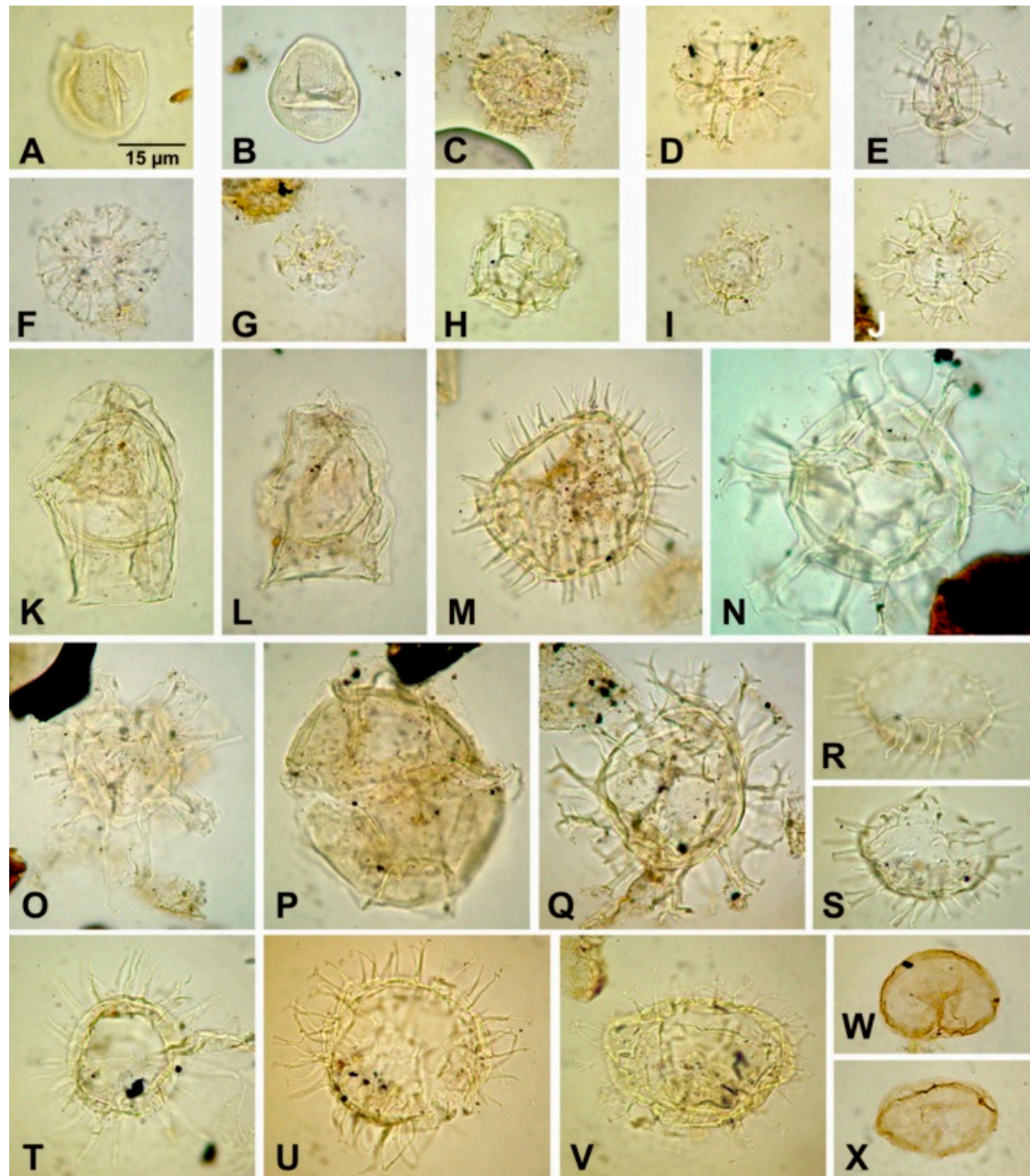


**Figure 5.** Dinoflagellate cysts from the Babczyn 2 borehole. **A** – *Batiacasphaera sphaerica*, sample 8; **B** – *Pyxidiniopsis psilata*, sample 8; **C** – *Labyrinthodinium truncatum*, sample 9; **D** – *Reticulatosphaera actinocoronata*, sample 9; **E** – *Melitasphaeridium pseudorecurvatum*, sample 11; **F** – *Nematosphaeropsis labyrinthus*, sample 11; **G** – *Cordosphaeridium minimum*, sample 15; **H** – *Impagidinium* sp., sample 19; **I** – *Impagidinium* sp., sample 23; **J** – *Spiniferites ramosus* s.l., sample 23; **K** – *Hystrichosphaeropsis obscura*, sample 11; **L** – *Hystrichosphaeropsis obscura*, sample 11; **M** – *Operculodinium centroparpum*, sample 11; **N** – *Spiniferites pseudofurcatus*, sample 15; **O** – *Hystrichokolpoma rigaudiae*, sample 15; **P** – *Pentadinium laticinctum*, sample 11; **Q** – *Spiniferites ramosus* s.l., sample 21; **R, S** – *Polysphaeridium subtile*, same specimen, various foci; sample 27; **T** – *Lingulodinium machaerophorum*, sample 23; **U** – *Systematophora placacantha*, sample 27; **V** – *Systematophora ?ancyrea*, sample 41; **W** – *Selenopemphix nephroides*, sample 41; **X** – *Selenopemphix nephroides*, sample 41. Scale bar in **A** refers to all photomicrographs.

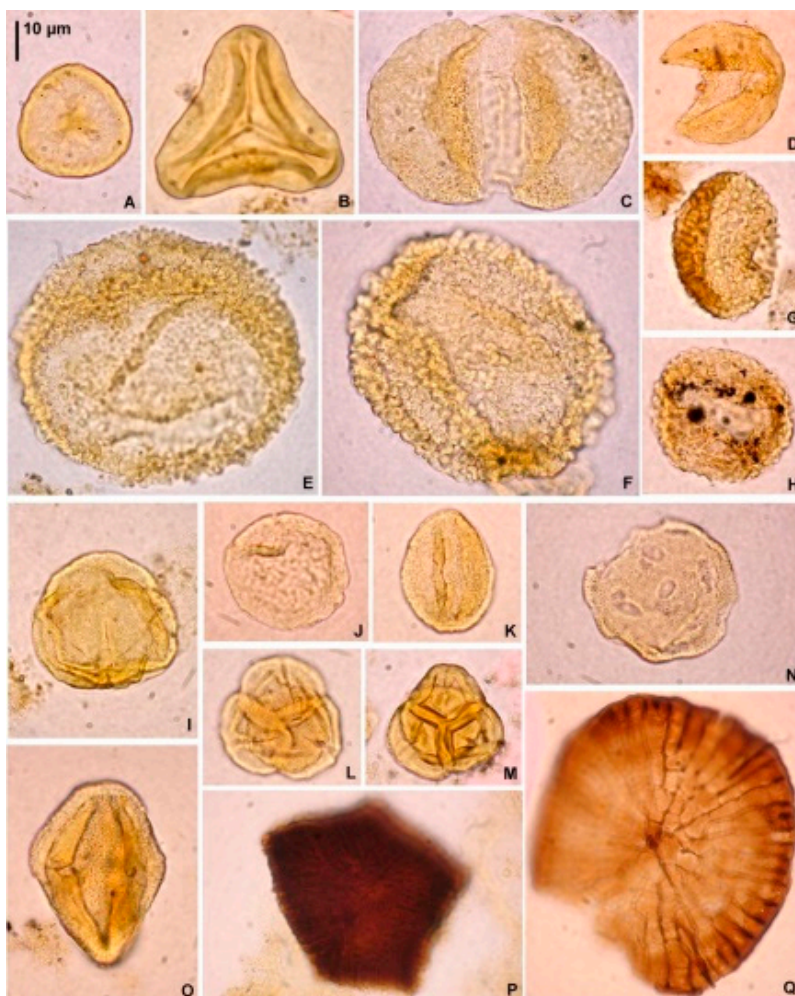


**Figure 6.** Terrestrial palynomorphs from the Babczyn 2 borehole. **Spores of plants:** **A** – *Stereisporites* sp., sample 55; **B** – *Neogenisporis* sp., sample 55; **Pollen grains:** **C** – *Cathayapollis* sp., sample 47; **D** – *Inaperturopollenites* cf. *verrucapillatus* Trevisan, sample 47; **E** – *Zonalapollenites gracilis* Krutzsch, sample 47; **F** – *Zonalapollenites verrucatus* Krutzsch, sample 55; **G** – *Sciadopityspollenites verticillatiformis* (Zauer) Krutzsch, sample 15; **H** – *Sciadopityspollenites verticillatiformis* (Zauer) Krutzsch, sample 33; **I** – *Faguspollenites* sp., sample 43; **J** – *Ulmipollenites undulosus* Wolff, sample 47; **K** – *Quercopollenites* sp., sample 55; **L** – *Ericipites baculatus* Nagy, sample 33; **M** – *Ericipites* sp., sample 55; **N** – *Periporopollenites orientalisformis* (Nagy) Kohlman-Adamska & Ziemińska-Tworzydło, sample 17; **O** – *Edmundipollis* sp., sample 9; **Fungi:** **P** – *Cephalothecoidomyces* cf. *neogenicus* G. Worobiec, Neumann & E. Worobiec, sample 47; **Q** – *Phragmothyrites* sp., sample 15. Scale bar in **A** refers to all photographs.

A Zeiss Axiolab microscope equipped with 20x lens and 100x oil lens was used for the analyses of palynofacies and dinoflagellate cysts. Quantitative dinoflagellate cyst analysis was done by counting to about 300 specimens; in lower frequency cases, all specimens from the both prepared slides were counted. On this basis, the Shannon–Weaver diversity index ( $H'$ ) was calculated as:  $H' = -\sum p_i \ln(p_i)$ , where  $p_i$  is the relative abundance of each taxon, and expressed as  $e^{H'}$ . The most frequent and important taxa for palaeoenvironmental reconstructions were grouped into eight dinoflagellate cyst morphogroups:

- *Spiniferites* morphogroup: including all *Spiniferites* and *Achomosphaera* specimens;
- *Batiacasphaera* morphogroup: including *B. sphaerica*, *B. sp. A*, *B. micropapillata*, and *B. hirsuta*;
- *Operculodinium* morphogroup: including all *Operculodinium* specimens;
- *Systematophora* morphogroup: includes *S. placacantha* and *S. ?ancyrea* specimens. The latter differed from *S. placacantha* due to incomplete or absent proximal ridges;
- *Lingulodinium* morphogroup: including *Lingulodinium machaerophorum* and a single specimen of *Lingulodinium* sp. A;

- *Nematosphaeropsis* morphogroup: including *N. labyrinthus*;
  - *Impagidinium* morphogroup: including *Impagidinium* sp. and *I. striatum* specimens.
  - *Polysphaeridium* morphogroup: including *P. subtile* and *P. zoharyi*;
- The palynofacies analysis was performed by counting to 500 particles. The palynofacies elements in the present study were assigned to nine groups:
- Black, opaque phytoclasts representing the most resistant, coalified, land plant remains;
  - Dark brown phytoclasts, which are land plant remains, usually equidimensional, translucent (or with translucent edges), remaining in structureless wood or cortical tissue;
  - Cuticle group, including structured land plant tissue remains with usually preserved cell structure; these are commonly the remains of the leaf epidermis;
  - Pollen grains of angiosperms and gymnosperms; the most common are bisaccate pollen grains of gymnosperms;
  - Pteridophyte spores;
  - Dinoflagellate cysts;
  - Algae and acritarch group, including algae other than dinoflagellate cysts, such as Prasinophyte (e.g., *Tasmanites*, *Cymatiosphaera*, and *Leiosphaera*), and *incertae sedis* microfossils (i.e., acritarchs);
  - Foraminifera organic linings (zooclasts), which are the organic cells of foraminifera;
  - Amorphous organic matter (AOM), which represents structureless particles of uncertain origin (most likely marine in the case of the present study material) being a stage of bacterial decay of organic particles in oxygen-depleted environment.

The identified sporomorph taxa were classified on the basis of the "Atlas of pollen and spores of the Polish Neogene" [44–47]. In the studied material, the following palaeofloristical elements were distinguished: "palaeotropical" (P), including: "tropical" (P1) and "subtropical" (P2); "arctotertiary" (A), including: "warm-temperate" (A1) and "temperate" (A2); and cosmopolitan (P/A). The data from the palynological spectra were used to construct a palynological diagram. In the diagram the percentage shares of the pollen and spore taxa were calculated from the total sum of pollen grains and spores, and the proportion of non-pollen palynomorphs was computed separately in relation to the total sum using the POLPAL software [48].

Microphotographs of selected sporomorphs and fungal palynomorphs (Figure 6) were obtained using a Nikon Eclipse E400 microscope equipped with a Canon A640 digital camera.

### 3. Results

#### 3.1. Foraminifera

The Babczyn 2 succession contains well-preserved planktonic, calcareous benthic, and agglutinated foraminifera (Appendix 1 in [8]). Altogether 60 species, representing the following genera: *Articulina*, *Cycloforina*, *Pseudotriloculina*, *Quinqueloculina*, *Sigmoilinita*, *Triloculina*, *Varidentella*, *Elphidium*, *Haynesina*, *Porosonion*, *Anomalinoidea*, *Heterolepa*, *Hanzawaia*, *Lobatula*, *Cibicidoides*, *Elphidiella*, *Melonis*, *Nonion*, *Pullenia*, *Bolivina*, *Bulimina*, *Uvoigerina*, *Angulogerina*, *Sphaeroidina*, *Favulina*, *Globigerina*, *Velapertina*, *Trilobatus*, *Ammobaculites*, *Ammodiscus*, *Martinottiella*, *Siphotextularia*, *Textularia*, *Spirorutilus*, *Pavonitina*, *Pseudogaudryina*, *Rhabdammina*, and *Nothia*.

In the Badenian part of the studied succession comprising the Pecten Beds and lowermost part of the Syndesmya Beds, both planktonic and benthic foraminifera occur. However, in sample 9 tests of foraminifera are damaged in most cases what indicates their transportation and reworking. Sample 10 possesses almost entirely planktonic foraminifera; rare specimens of a few benthic foraminifera were recorded. Samples 11 to 28 yielded abundant and well preserved foraminiferal assemblages, and sample 29 is devoid of foraminifera. Upsection, the samples 30 to 35 from the lowermost Sarmatian yielded only benthic foraminifera, and in the upper part of the section (samples 35 to 55) foraminifera are rare and their assemblage is composed of miliolids and reworked forms from the Badenian. Only in a short interval (samples 47 to 49) abundant assemblage of miliolids occurs, and in samples 50 and 51 *Bolivina sarmatica* with miliolids is recorded. Due to small numbers of specimens, quantitative analysis was not performed for the upper part of section studied.

The following genera exceed 5% at least in one sample: *Bulimina*, *Bolivina*, *Uvigerina*, *Angulogerina*, *Cibicidoides*, *Melonis*, *Sphaeroidina*, *Hanzawaia*, *Spirorutilus* and *Heterolepa* (Figure 7). Quantitative analysis enabled to group samples with homogeneous foraminiferal assemblages. Nine foraminiferal assemblages were recognized in the lower part of the interval studied (Figure 7).

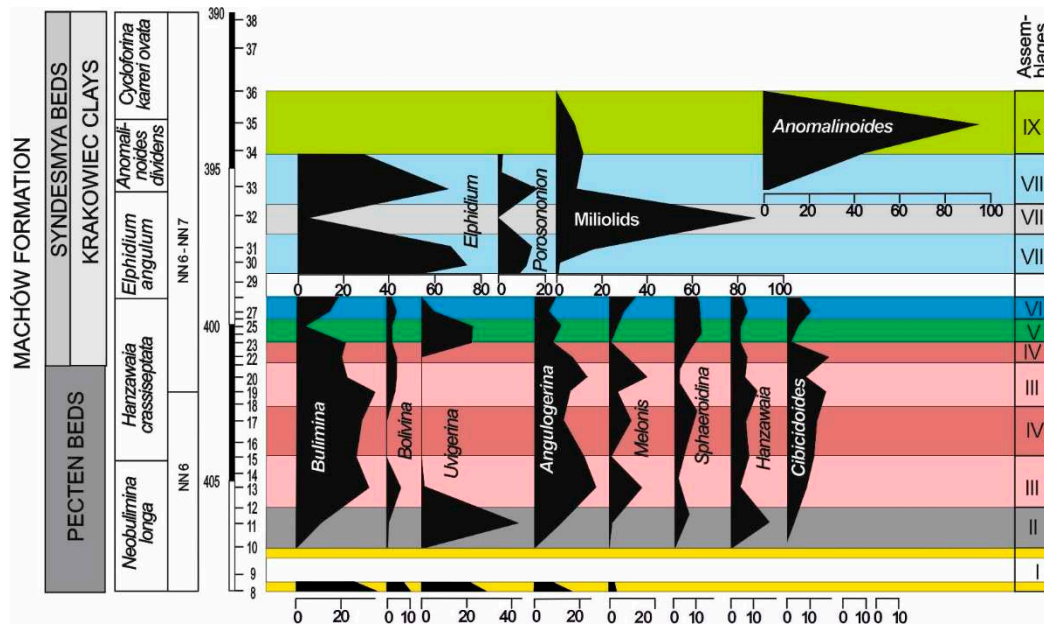


**Figure 7.** Relative abundance of the most common benthic foraminiferal genera (in percent) of the Babczyn 2 borehole.

Assemblage I occurs at the base of the section (samples 8 and 10; sample 9 due to large numbers of resedimented specimens has not been taken into account) (Figure 7). This assemblage is characterized by a dominance of *Bulimina* (30%) and *Uvigerina* (30%). Other important components are *Angulogerina* which exceeds 17% and *Bolivina* (10%). Subsidiary species include: *Melonis pompilioides*, *Globocassidulina subglobosa*, *Astrononion perfossum*, *Asterigerinata planorbis*, *Lobatula lobatula*. P/B ratio exceeds 60%.

The presence of planktonic foraminifera, mainly *Globigerina*, in this assemblage indicates a normal salinity marine environment of the inner to middle shelf depths [49,50]. Moderate benthic foraminiferal diversity [18 species, H(S) diversity index 2.5] and predominance of infaunal morphogroups (>90%) (Figure 4) within benthic foraminifera suggests suboxic to dysoxic bottom waters.

Assemblage II is recorded in sample 11 (Figure 7). It is dominated by *Uvigerina* which reaches 40% in the benthic foraminiferal assemblage. *Bulimina* and *Angulogerina* slightly exceed 10% (11 and 12%, respectively). *Hanzawaia* (16%) and *Cibicidoides* (6%) are other common components of this assemblage. P/B only 17%, H(S) diversity index 2.5 and significant drop of infaunal morphogroups in the assemblage to 70% (Figure 4) suggest a shallowing of the sea and amelioration of oxic conditions in the bottom waters. Assemblage III occurs in samples 13, 19, 20 (Figure 7). It is dominated by *Bulimina* (30% to 40%), *Angulogerina* (16% to 28%) and *Melonis* (14% to 17%). Minor components of the assemblage are *Bolivina*, *Cibicidoides*, *Sphaeroidina*, *Hanzawaia*. P/B vary from 70% to 85%; H(S) is comprised between 2.3 and 2.7; infaunal species compose 75% of the assemblage (Figure 4).

Assemblage IV is recorded in samples 15, 17, 22 (Figure 7). *Bulimina* (20% to 34%), *Angulogerina* (12% to 17%) and *Sphaeroidina* (7% to 10%), *Cibicidoides* – 13%, *Hanzawaia* – 8%. In this assemblage, for the first time in the studied interval, appear agglutinated foraminifera: *Spirorutilus*, *Siphotextularia*, *Ammodiscus*. P/B is high and reaches 65%; H(S) is 2.6 to 2.7; infaunal species compose 60 to 70% of the assemblage (Figure 4).

Assemblages III and IV alternate twice in the middle and upper part of the Pecten Beds. They differ from under- and overlying assemblages by a complete lack of *Uvigerina*. Instead, *Angulogerina angulosa* is one of dominant taxa and forms 12% to 28% of these assemblages.

The next assemblage V occurs in samples 23 and 25 (Figure 7). In these samples *Uvigerina* reappeared and it forms >20% of the assemblage. The content of three other species is around 10%: *Heterolepa dutemplei* (10%), *Angulogerina angulosa* (8-10%) and *Sphaeroidina bulloides* (12%). P/B is about 25%, H(S) diversity index 2.8 and infaunal morphogroups in the assemblage form 80% (Figure 4)

Assemblage VI is recorded in samples 27 and 28 (Figure 7). *Bulimina* forms 15 to 19% while *Uvigerina* drops to 0–6%. *Angulogavelinella angulosa* forms 6 to 9%, *Sphaeroidina bulloides* 8 to 10%, *Heterolepa dutemplei* 5 to 7%, and agglutinated forms form 13% of the assemblage (*Siphotextularia inopinata* – 10% and *Spirorutilus carinatus* – 3%). P/B is low, from 22 to 27%; H(S) is 2.9 to 3.0; infaunal species compose 65 to 70% of the assemblage (Figure 4). This abundant, highly diversified foraminiferal assemblage suddenly disappeared at 399.4 m depth (sample 28).

Sample 29 is almost barren of foraminifera; it yields only rare specimens of small-sized elphidiids (*E. angulatum*), *Porosonion martkobi*, *Nonion tumidulus* and miliolids (*Cycloforina predkarpatica*, *Varidentella reussi*) and a few reworked specimens of foraminifera from upper Badenian strata.

Assemblage VII is recorded in samples 30, 31 and 33 (Figure 7). It is dominated by *Elphidium* which form 60 to almost 80% of the assemblage; *Porosonion* and miliolids form 10 to 20%. H(S) is 1.8 to 1.9; infaunal species account for less than 35% (Figure 4).

Assemblage VIII occurs in samples 32, 47, 48, and 49 (Figure 7). It is very low diversified, almost completely composed by miliolids assemblage. H(S) is 0.77; only epifauna occurs (Figure 4).

Assemblage IX is recorded in samples 34 and 35 (Figure 7). It is almost monospecific assemblage of *Anomalinoidea dividens*. (50 to 90%). Miliolids form 8 to 12%, and H(S) is 0.33 to 1.8 (Figure 4).

### 3.2. Palynofacies

All samples yielded palynological organic matter, the elements of which showed various ratios reflecting variable environmental conditions and/or various sedimentological processes (Figure 8). The palynofacies of the studied samples were dominated by terrestrial elements represented by palynodebris (black and dark brown phytoclasts and cuticles) and pollen grains. The share of these two groups showed variable proportions: palynodebris (cuticles in particular), dominate in the lower part of the studied interval, and decreased upwards, being replaced by pollen grains (in the middle part) and AOM in the upper part (Figure 8).

The proportion of marine elements (dinoflagellate cysts – Figure 5, prasinophytes, acritarchs, and rare zooclasts) rarely exceeded 10%. Dinoflagellate cysts were most common in the lower and middle intervals, while becoming rare or absent in the upper part, where prasinophytes and acritarchs predominate among the aquatic palynomorphs (Figure 8).

AOM occurs in two samples from the middle part of the studied interval (samples 29 and 31) and in the upper part, where it dominated in some samples (Figure 8).

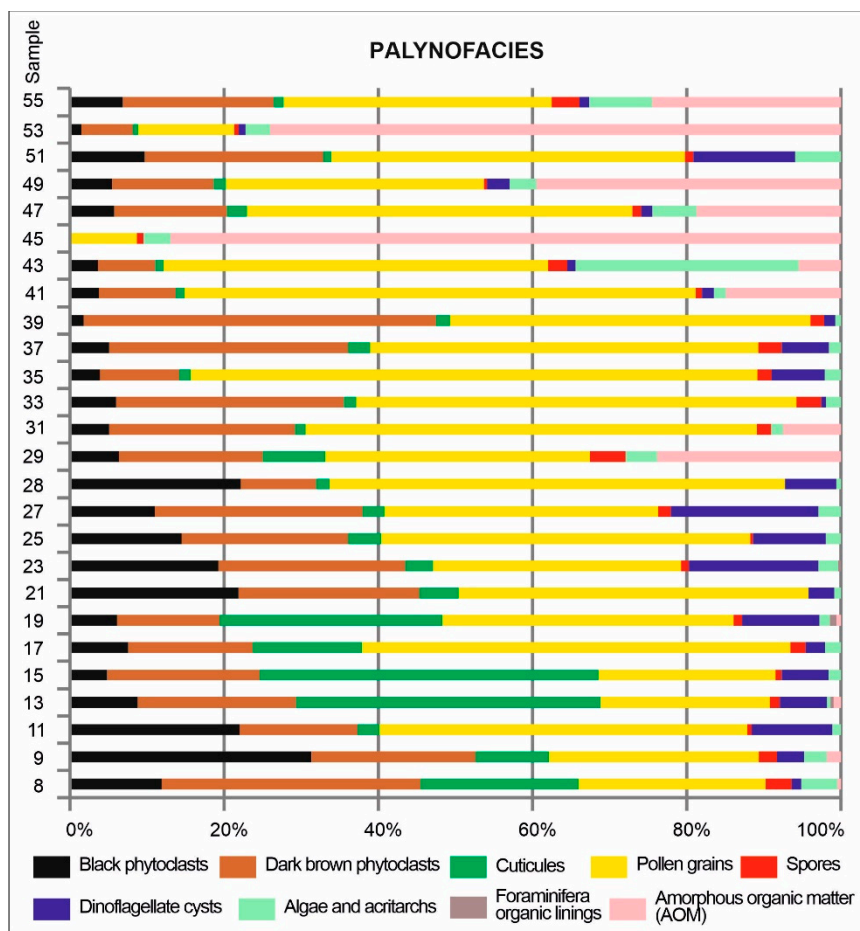


Figure 8. Palynofacies changes in the Babczyn 2 borehole.

### 3.3. Dinoflagellate cysts

Virtually all the studied samples (except for samples 29, 31, and 45) involved dinoflagellate cysts. A total of 44–48 taxa assumed to be in situ were distinguished. We note that some taxa, such as *Spiniferites ramosus* s.l., included several species and/or subspecies, which were not distinguished for the purposes of the present study (Table 1). Despite this apparent taxonomical richness, the taxonomic diversity of the dinoflagellate cyst assemblages was low, and it oscillated between 2.0 and 6.5 (Figure 9). The majority of samples yielded assemblages dominated by three to four species, with the remaining taxa being represented by rare or even single specimens. The dominant taxa included *Operculodinium* spp. and *Lingulodinium machaerophorum*; their proportions varied from sample to sample and could also be different in neighbouring samples. Some species, like *Nematosphaeropsis labyrinthus*, *Selenopemphix nephroides*, *Reticulatosphaera actinocoronata*, *Lingulodinium machaerophorum*, and *Polysphaeridium subtile*, showed increased frequencies only in single samples.

The highest diversity values between 4.5 and 6.5 were recorded in the lower studied interval, which included the upper Badenian (samples 8–27, except for samples 17 and 25). Diversity decreased in the succession, above the two barren samples 29 and 31, where it oscillated between 2.3 and 4.5 (with the minimal diversity of 0.5 being recorded in sample 51). However, this decreasing upwards diversity trend was not gradual; a characteristic feature was that the diversity of assemblages from the subsequent samples were alternately higher and lower, thereby forming the zigzag course of the chart (Figure 9). The diversity of dinoflagellate cyst assemblages was generally correlated with the number of taxa. The highest numbers of dinoflagellate cysts (15–22) were recorded in the lower part of the studied interval (samples 9–27). The number of taxa from the higher interval was lower,

oscillating between 4 and 7, with higher values (i.e., 11, 13 and 16) being present only in three samples (37, 35 and 49, respectively; Figure 9).

Another characteristic feature of the dinoflagellate cyst assemblages from the studied borehole interval was the predominance of gonyaulacoids. Most of studied samples yielded purely gonyaulacoid assemblages. Peridinioids were represented by *Selenopemphix* and *Lejeunecysta*; the latter and *S. brevispinosa* occurred mainly as single specimens only in a few samples (Table 1), whereas *S. nephroides* formed an acme in sample 41 (up to 25% of the whole assemblage; Figure 9).

The diversity and frequency of taxa in the studied material were related to the frequencies of some taxa grouped into eight morphogroups. Representatives of the Spiniferites and Batiacasphaera morphogroups were the most common taxa in the lower part of the studied succession (samples 8–28). Their frequencies showed a negative correlation: samples with common Spiniferites yielded few Batiacasphaera, whereas increased frequencies of Batiacasphaera were associated with decreased Spiniferites (Figure 9). This relationship was further correlated with changes in diversity in this interval; Batiacasphaera-dominated assemblages (samples 17, 21, and 25) showed the lowest diversities. Representatives of the Batiacasphaera morphogroup were virtually absent in the upper interval (Table 2); the only exception was their common occurrence in sample 51, which yielded the most taxonomically impoverished assemblage (Figure 9).

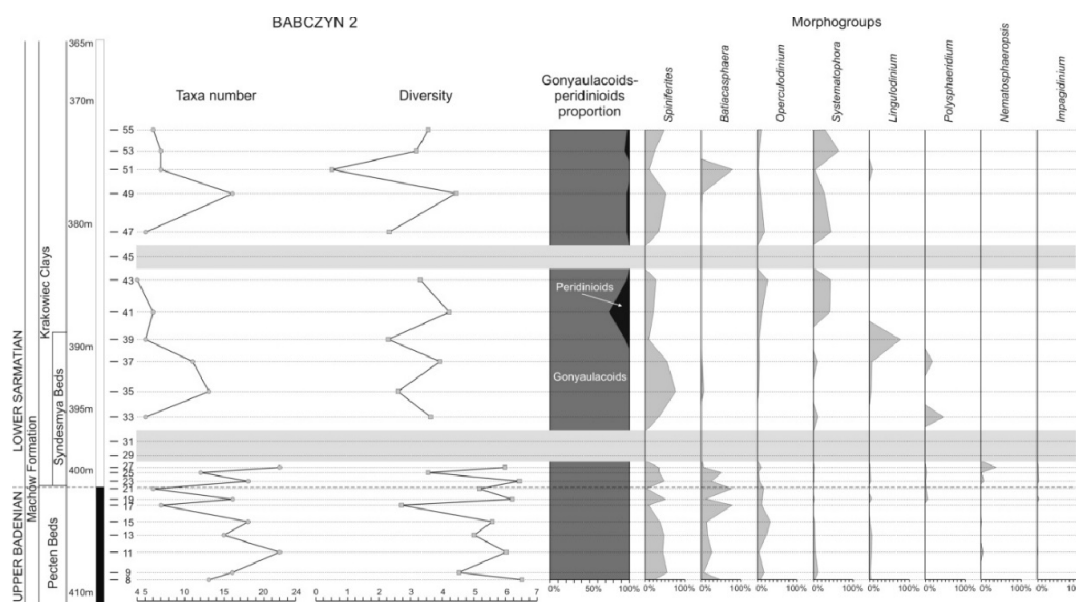


**Figure 9.** Palaeoenvironmental proxies of aquatic palynomorphs from the Babczyn 2 borehole.

**Table 1.** Distribution of aquatic palynomorphs in the Babczyn 2 borehole; (\*) indicates reworked specimens; their occurrence is not included in a total count.

	Age	Upper Badenian											
		Machów Formation											
		Pecten Beds								Syndesmya Beds			
	Sample	8	9	11	13	15	17	19	21	23	25	27	28
	<i>DINOFLAGELLATE CYSTS</i>												
1.	<i>Pentadinium laticinctum</i>	13		1	2	2				1		4	1
2.	<i>Batiacasphaera sphaerica</i>	68	3	3	4	5	3	1	20	22		3	2
3.	<i>Spiniferites ramosus s.l.</i>	81	162	135	120	117	5	138	2	153	65	109	128
4.	<i>Batiacasphaera sp. A</i>	79	12	87	43	41	44	32	16	51		1	

5.	<i>Operculodinium centrocarpum</i>	27	51	5	59	96	5	37	9	18	3	25	29
6.	<i>Melitasphaeridium?pseudorecurvatum</i>	3											
7.	<i>Homotryblium tenuispinosum*</i>	*				*		*					
8.	<i>Melitasphaeridium choanophorum</i>	4		15	3	13		4		6		3	12
9.	<i>Pyxidinospis psilata</i>	7		3	1		1			2		1	12
10.	<i>Systematophora placacantha</i>	6	41	16	10	12		5		2	1	7	3
11.	<i>Lingulodinium machaerophorum</i>	9	5	11	14	2		15		12	3	5	
12.	<i>Labyrinthodinium truncatum</i>	5	10	12		7		2				2	2
13.	<i>Reticulosphaera actinocoronata</i>	1	3	5	1	6		18		6		2	
14.	<i>Dapsilidinium</i> sp.	2											
15.	<i>Operculodinium</i> sp. C		2										
16.	<i>Spiniferites pseudofurcatus</i>		1	2	1	3		5					
17.	<i>Hystrihostrogylon</i> sp.		1										
18.	<i>Reticulosphaera?</i> sp.		1										
19.	<i>Spiniferites</i> sp. A		3	4	4			2		2	3	3	6
20.	<i>Lejeunecysta</i> sp.		1								1	2	
21.	<i>Hystrihostrophaeropsis obscura</i>		1	4									
22.	<i>Pyxidinospis?</i> sp.		1			1							
23.	<i>Cordosphaeridium</i> cf. <i>minimum</i>			2		1				8		1	
24.	<i>Melitasphaeridium pseudorecurvatum</i>			1	1	1	1	1			4	1	
25.	<i>Nematosphaeropsis labyrinthus</i>			6		1				15	1	119	
26.	<i>Cerodinium</i> sp.*			*									*
27.	<i>Homotryblium plectilum*</i>			*								*	*
28.	<i>Impagidinium</i> sp.			1		1		6		5		1	
29.	<i>Hystrihostrokolpoma rigaudiae</i>			2	1	1							2
30.	<i>Cordosphaeridium minimum</i>			1		1				1		3	
31.	<i>Operculodinium</i> sp. B			4		2							
32.	<i>Wetzeliella</i> sp.*			*									*
33.	<i>Charlesdowniea</i> sp.*			*									
34.	<i>Operculodinium</i> sp. A			1	2		1						

	Age	Lower Sarmatian													
		Machów Formation													
		Syndesma Beds						Krakowiec Clays							
Sample	29	31	33	35	37	39	41	43	47	4	51	53	55		
1.	<i>Pentadinium laticinctum</i>			3	1	2					1	1			
2.	<i>Batiacasphaera sphaerica</i>				9						1				
3.	<i>Spiniferites ramosus</i> s.l.			12	242	135	3	25	24	52	1	4	12	31	50







Lingulodinium share was similar: it was infrequent or absent being a dominant taxon (almost 80%) in sample 39.

Nematosphaeropsis labyrinthus was a very rare species throughout the studied borehole interval; it occurred infrequently in only four samples from the basal part (Table 2). However, it formed an acme in the sample 27, collected below the barren interval (samples 29 and 31), where it reached almost 40% of all dinoflagellate cysts.

Impagidinium morphogroup is another group, whose representatives occurred in the basal part of the studied borehole interval (only one specimen was found in the remaining part, sample 49). The distribution of very uncommon specimens of Impagidinium showed a pattern similar to that of Nematosphaeropsis (Figure 9).

#### 3.4. Other aquatic palynomorphs

Dinoflagellate cysts were not the only aquatic palynomorphs found in the studied borehole interval. Other aquatic palynomorphs occurred in all the samples, while reaching even high frequencies in some of them. These included acritarchs (e.g., Veryhachium, Nannobarbophora, and unidentified small, sphaeromorphic, spiny and smooth forms), prasinophytes (e.g., Tasmanitaceae and Leiosphaeridiaceae), and zooclasts (foraminifera organic linings, scolecodonts, and remains of presumably arthropods). The diversity of other aquatic palynomorphs exhibited high variability from sample to sample, thereby resembling the distribution pattern of dinoflagellate cyst assemblages.

The lowermost sample (no. 8), yielded frequent Leiosphaeridiaceae (described below as the genus Leiosphaeridia, although its precise taxonomic position is tentative). Samples 9–13 yielded foraminifera organic linings and Nannobarbophora. Tasmanites co-occurred with Nannobarbophora in sample 15 and Leiosphaeridia in sample 17. Neither samples yielded foraminifera organic linings; these were found in sample 19 (with frequent Nannobarbophora and rare Leiosphaeridia). The latter had increased frequency in the subsequent sample, sample 21, which yielded no Nannobarbophora and only single foraminifera organic linings. The frequency of Leiosphaeridiaceae in higher samples showed a fluctuating course: it decreased in sample 23, increased in sample 25 and decreased again in sample 27, whereas the occurrences of Tasmanites and Nannobarbophora in these samples showed the opposite trend. Sample 27 yielded also Veryhachium. Rare Tasmanites and Veryhachium were the only prasinophytes and acritarchs in sample 28.

The distribution pattern of acritarchs and prasinophytes in the lower part of the studied borehole interval (samples 8–28) showed a specific pattern that was further correlated with dinoflagellate cyst assemblages. There was a clear negative correlation between the assemblages dominated by foraminifera organic linings and Nannobarbophora (and Tasmanites to a lesser degree) and those dominated by Leiosphaeridia. Moreover, the samples that yielded the former assemblages yielded relatively diverse dinoflagellate cyst assemblages. These samples, which yielded impoverished assemblages dominated by Batiacasphaera, also exhibited increased frequencies of Leiosphaeridia.

Various spherical forms attributed here to Leiosphaeridiaceae became the nearly sole aquatic palynomorphs in samples 29 and 31, which yielded no dinoflagellate cysts; scolecodonts were found in sample 31. Leiosphaeridia were again dominant in the subsequent sample 33, which yielded impoverished dinoflagellate cyst assemblages with relatively frequent Polysphaeridium.

Higher intervals of the studied borehole (samples 35–55) yielded common to very common Leiosphaeridiaceae, represented by morphologically diversified forms, some of which likely representing sphaeromorphic, smooth acritarchs. They were predominant in these samples over other prasinophytes, and acritarchs were commonly the only aquatic palynomorphs (other than dinoflagellate cysts). Rare Nannobarbophora occurred in samples 35, 37, and 49, and a single foraminifera organic lining was found in sample 51.

Reworked dinoflagellate cysts commonly occurred in the lower part of the studied borehole interval (samples 8–28). These were Palaeogene specimens representing mainly Eocene–Oligocene forms, and the Palaeohystrichophora found in sample 27 may have been Cretaceous forms. Higher

borehole intervals yielded much less frequently reworked specimens, which were mainly Cretaceous forms (Table 2; reworked taxa are highlighted with an asterisk).

### 3.5. Spore-pollen analysis

All samples yielded pollen grains and spores suitable for palynological analysis. In most samples, 300–500 pollen grains and spores (min. 100 in sample 21) were identified. Besides sporomorphs, all co-occurring non-pollen palynomorphs in the samples were counted. Most sporomorphs were poorly preserved; however, they were still identifiable. A total of 71 fossil-species (including nine species of plant spores, 16 species of gymnosperm pollen, and 46 species of angiosperm pollen) were identified (Table 2). In all samples, among the pollen grains of gymnosperms, bisaccate pollen grains (Figure 6C) of the Pinaceae family (mainly *Pinus*, plus *Cathaya*, *Abies*, *Picea*, *Keteleeria/Pseudolarix*, and *Cedrus*), *Taxodium/Glyptostrobus* (Figure 6D), *Tsuga* (Figure 6E, F), and *Sciadopitys* (Figure 6G, H) were the most common. Additionally, several pollen grains of *Sequoia/Sequoiadendron/Meta-sequoia/Cryptomeria* were encountered (Figure 10).

Among the angiosperm pollen grains of *Fagus* (Figure 6I), *Ericaceae* (Figure 6L, M), *Quercus* (fossil genus *Quercopollenites* – Figure 6K – and fossil species *Quercoidites henricii*), *Ulmus* (Figure 6J), *Pterocarya*, *Carya*, *Zelkova*, *Liquidambar* (Figure 6N), *Alnus*, and *Myrica* were the most common. Pollen grains of *Acer*, *Carpinus*, fossil-species *Tricolporopollenites pseudocingulum*, *Tilioideae*, *Betula*, *Celtis*, and *Juglans* were regularly observed in the samples. *Ilex* and *Nyssa* were mainly present in samples from the lower section of the profile. In addition, a few pollen grains of *Adoxaceae*, *Castanea/Castanopsis/Lithocarpus*, *Cercidiphyllum*, *Cyrillaceae/Clethraceae*, *Eucommia*, *Fraxinus*, *Salix*, *Symplocos* as well as the fossil-species *Edmundipollis* sp. (Figure 6O), *Parthenopollenites marcodurensis*, *Tricolporopollenites fallax*, *T. indeterminatus*, and *T. liblarensis* were encountered. Herbs were very rare, represented by members of the *Chenopodiaceae*, *Cyperaceae*, *Poaceae*, and *Sparganiaceae/Typhaceae* families (Tab. 2, Figure 10).

Fern spores were also rare, with the *Baculatisporites*, *Laevigatosporites*, *Leiotriletes*, *Neogenisporis* (Figure 6B), and *Verrucatosporites* fossil genera being present. In contrast, spores of *Sphagnum* (Figure 6A) were encountered in all samples. Several lycopod spores (related to the modern genera *Lycopodium* and *Lycopodiella*) were also recorded. Typical freshwater algae were virtually absent, and only scarce *Botryococcus* colonies were encountered. Microremains of fungi (Figure 6P, Q) were continually found in the palynological profile. Fungal spores were present in all the samples, whereas sporocarps were mainly present in the upper section of the profile (Figure 10).

**Table 2.** Spores and pollen grains recorded in samples from the Babczyn 2 borehole. Taxonomy and botanical affinity according to Stuchlik et al. (2001, 2002, 2009, 2014). The following palaeofloristical elements have been distinguished: palaeotropical (P), including: tropical (P1) and subtropical (P2), and “arctotertiary” (A), including: warm-temperate (A1) and temperate (A2), as well as cosmopolitan (P/A).

FOSSIL TAXON	BOTANICAL AFFINITY	ELEMENT
<i>Spores of plants:</i>		
<i>Baculatisporites</i> sp.	Osmundaceae: <i>Osmunda</i>	P/A
<i>Camaronosporites</i> sp.	Lycopodiaceae: <i>Lycopodiella</i> sect. <i>Campylostachys</i>	P
<i>Distoverrusporis</i> sp.	Sphagnaceae: <i>Sphagnum</i>	P/A
<i>Laevigatosporites</i> sp.	Polypodiaceae, Davalliaceae, and other ferns	P/A
<i>Leiotriletes</i> sp.	Lygodiaceae and other ferns	P
<i>Neogenisporis</i> sp.	Gleicheniaceae, Cyatheaceae	P1
<i>Retitriletes</i> sp.	Lycopodiaceae: <i>Lycopodium</i>	A

<i>Stereisporites</i> sp.	Sphagnaceae: <i>Sphagnum</i>	P/A
<i>Verrucatosporites</i> sp.	Davalliaceae, Polypodiaceae, and other ferns	P/A
<b>Pollen grains of gymnosperms:</b>		
<i>Abiespollenites</i> sp.	Pinaceae: <i>Abies</i>	A
<i>Cathayapollis</i> sp.	Pinaceae: <i>Cathaya</i>	A1
<i>Cedripites</i> sp.	Pinaceae: <i>Cedrus</i>	A1
<i>Inaperturopollenites concedipites</i> (Wodehouse) Krutzsch	Cupressaceae: <i>Taxodium</i> , <i>Glyptostrobus</i>	P2/A1
<i>Inaperturopollenites verrucapapillatus</i> Trevisan	Cupressaceae: <i>Taxodium</i> , <i>Glyptostrobus</i>	P2/A1
<i>Keteleeriapollenites</i> sp.	Pinaceae: <i>Keteleeria</i> , <i>Pseudolarix</i>	A1
<i>Piceapollis praemarianus</i> Krutzsch	Pinaceae: <i>Picea</i>	A
<i>Piceapollis</i> sp.	Pinaceae: <i>Picea</i>	A
<i>Pinuspollenites labdacus</i> (Potonié) Raatz	Pinaceae: <i>Pinus sylvestris</i> type	A
<i>Pinuspollenites</i> sp.	Pinaceae: <i>Pinus</i>	A
<i>Sciadopityspollenites verticillatiformis</i> (Zauer) Krutzsch	Sciadopityaceae: <i>Sciadopitys</i>	A1
<i>Sciadopityspollenites</i> sp.	Sciadopityaceae: <i>Sciadopitys</i>	A1
<i>Sequoiapollenites</i> sp.	Cupressaceae: <i>Sequoia</i> , <i>Sequoiadendron</i> , <i>Metasequoia</i>	A1
<i>Zonalapollenites gracilis</i> Krutzsch	Pinaceae: <i>Tsuga</i>	A
<i>Zonalapollenites verrucatus</i> Krutzsch	Pinaceae: <i>Tsuga</i>	A
<i>Zonalapollenites</i> sp.	Pinaceae: <i>Tsuga</i>	A
<b>Pollen grains of angiosperms:</b>		
<i>Aceripollenites</i> sp.	Sapindaceae: <i>Acer</i>	A1
<i>Alnipollenites verus</i> Potonié	Betulaceae: <i>Alnus</i>	P2/A
<i>Caprifoliipites</i> sp.	Adoxaceae: <i>Sambucus</i> , <i>Viburnum</i>	P/A1
<i>Carpinipites carpinoides</i> (Pflug) Nagy	Betulaceae: <i>Carpinus</i>	P2/A1
<i>Caryapollenites simplex</i> (Potonié) Raatz	Juglandaceae: <i>Carya</i>	A1
<i>Celtipollenites</i> sp.	Ulmaceae: <i>Celtis</i>	P/A1
<i>Cercidiphyllites minimireticulatus</i> (Trevisan) <i>Ziemińska-Tworzydło</i>	Cercidiphyllaceae: <i>Cercidiphyllum</i>	A1
<i>Chenopodipollis</i> sp.	Amaranthaceae (incl. Chenopodiaceae)	P/A
<i>Cupuliferoipollenites oviformis</i> (Potonié) Potonié	Fagaceae: <i>Castanea</i> , <i>Castanopsis</i> , <i>Lithocarpus</i>	P2/A1
<i>Cupuliferoipollenites pusillus</i> (Potonié) Potonié	Fagaceae: <i>Castanea</i> , <i>Castanopsis</i> , <i>Lithocarpus</i>	P2/A1
<i>Cyperaceapollis neogenicus</i> Krutzsch	Cyperaceae	P/A
<i>Cyrillaceapollenites megaexactus</i> (Potonié) Potonié	Cyrillaceae, Clethraceae	P
<i>Edmundipollis</i> sp.	Araliaceae, Cornaceae, Mastixiaceae	P/A
<i>Ericipites baculatus</i> Nagy	Ericaceae	A
<i>Ericipites ericius</i> (Potonié) Potonié	Ericaceae	A
<i>Ericipites</i> sp.	Ericaceae	A
<i>Eucommiapollis minor</i> Menke	Eucommiaceae: <i>Eucommia</i>	A1
<i>Faguspollenites</i> cf. <i>verus</i> Raatz	Fagaceae: <i>Fagus</i>	A
<i>Faguspollenites</i> sp.	Fagaceae: <i>Fagus</i>	A

<i>Fraxinipollis oblatu</i> Słodkowska	Oleaceae: <i>Fraxinus</i>	P/A
<i>Graminidites</i> sp.	Poaceae: Pooideae	P/A
<i>Ilexpollenites iliacus</i> (Potonié) Thiergart	Aquifoliaceae: <i>Ilex</i>	P/A1
<i>Ilexpollenites margaritatus</i> (Potonié) Thiergart	Aquifoliaceae: <i>Ilex</i>	P2
<i>Intratriporopollenites</i> sp.	Malvaceae: Tilioideae	P/A1
<i>Juglanspollenites</i> sp.	Juglandaceae: <i>Juglans</i>	A1/P2
<i>Myricipites</i> sp.	Myricaceae: <i>Myrica</i>	P2/A1
<i>Nyssapollenites</i> sp.	Nyssaceae: <i>Nyssa</i>	P2/A1
<i>Parthenopollenites marcodurensis</i> (Pflug & Thomson) Traverse	Vitaceae	P/A1
<i>Periporopollenites orientalisformis</i> (Nagy) Kohlman-Adamska & Ziemińska-Tworzydło	Altingiaceae: <i>Liquidambar</i>	A1
<i>Periporopollenites stigmosus</i> (Potonié) Thomson & Pflug	Altingiaceae: <i>Liquidambar</i>	A1
<i>Polyatriopollenites stellatus</i> (Potonié) Pflug	Juglandaceae: <i>Pterocarya</i>	A1
<i>Quercoidites henricii</i> (Potonié) Potonié, Thomson et Thiergart	Fagaceae: <i>Quercus</i>	P2/A1
<i>Quercopollenites rubroides</i> Kohlman-Adamska & Ziemińska-Tworzydło	Fagaceae: <i>Quercus</i>	A1
<i>Quercopollenites</i> sp.	Fagaceae: <i>Quercus</i>	A1
<i>Salixipollenites capreaformis</i> Planderová	Salicaceae: <i>Salix</i>	A
<i>Salixipollenites</i> sp.	Salicaceae: <i>Salix</i>	A
<i>Sparganiaceapollenites</i> sp.	Sparganiaceae, Typhaceae	P/A
<i>Symplocoipollenites vestibulum</i> (Potonié) Potonié	Symplocaceae: <i>Symplocos</i>	P
<i>Tricolporopollenites fallax</i> (Potonié) Krutzsch	Fabaceae	P/A
<i>Tricolporopollenites indeterminatus</i> (Romanowicz) Ziemińska-Tworzydło	Hamamelidaceae	P2
<i>Tricolporopollenites liblarensis</i> (Thomson) Hochuli	Fabaceae	P/A
<i>Tricolporopollenites pseudocingulum</i> (Potonié) Thomson & Pflug	Fagaceae?, Styracaceae?	P/A1
<i>Trivestibulopollenites betuloides</i> Pflug	Betulaceae: <i>Betula</i>	A
<i>Ulmipollenites undulosus</i> Wolff	Ulmaceae: <i>Ulmus</i>	A2
<i>Ulmipollenites</i> sp.	Ulmaceae: <i>Ulmus</i>	A2
<i>Zelkovaepollenites</i> sp.	Ulmaceae: <i>Zelkova</i>	A1

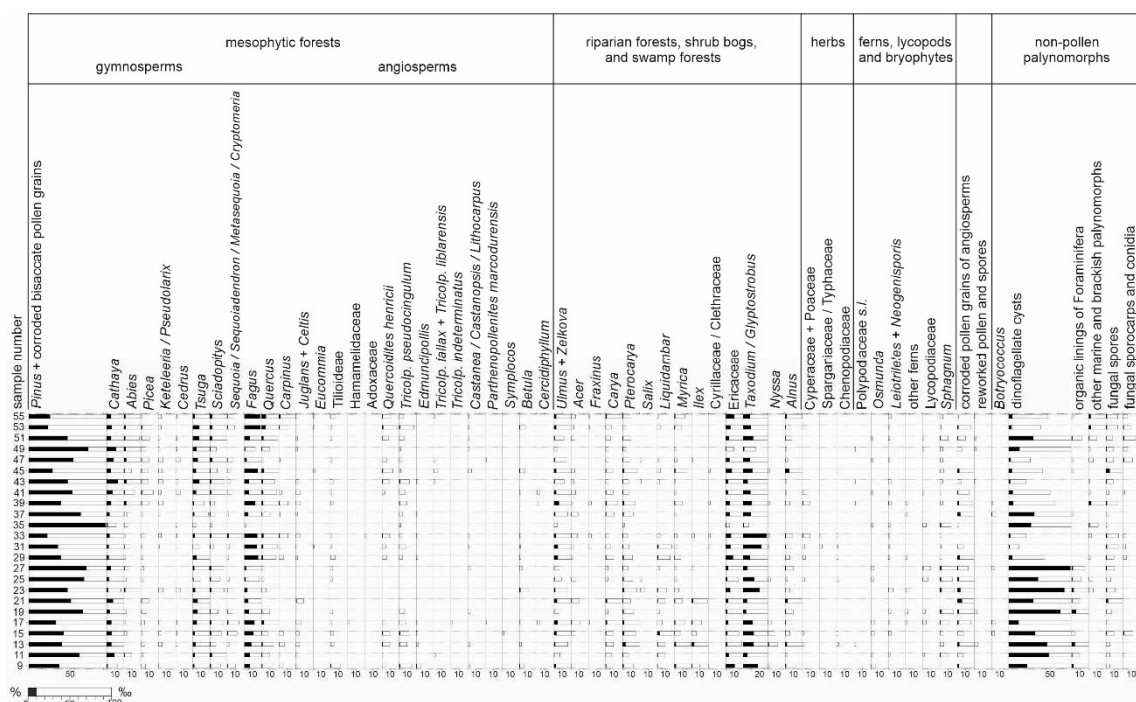


**Figure 10.** Palynological diagram from the Babczyn 2 borehole. Black bars show percentages (%), white bars show percentages  $\times 10$  (%o).

In all samples "arctotertiary" and cosmopolitan taxa prevailed, but "palaeotropical" and "palaeotropical/warm-temperate" taxa were also present (Tab. 2). "Palaeotropical" elements were represented by single specimens of *Camarozonosporites* sp., *Leiotriletes* sp., *Neogenisporis* sp., *Cyrtillaceapollenites megaexactus*, *Ilexpollenites margaritatus*, *Symplocoipollenites vestibulum*, and *Tricolporopollenites indeterminatus*. The representation of "palaeotropical/warm-temperate" taxa was more significant, and pollen grains of *Inaperturopollenites concedipites*, *I. verrupapillatus*, *Cupuliferoipollenites oviformis*, *C. pusillus*, *Ilexpollenites iliacus*, *Myricipites* sp., *Nyssapollenites* sp., *Parthenopollenites marcodurensis*, *Quercoidites henricii*, and *Tricolporopollenites pseudocingulum* occurred.

## 4. Discussion

### 4.1. Aquatic palaeoenvironment

Qualitative and quantitative analyses of foraminifera and aquatic palynomorphs showed that the studied borehole interval accumulated under variable, unstable sedimentary conditions.

Foraminifera are commonly used as proxies for palaeoenvironmental studies due to the correlation between foraminiferal test shapes and their palaeoenvironmental requirements. Planktonic foraminifera can be useful indicators of ancient sea level changes because of their depth stratification. Vertical distribution of planktonic foraminifers is directly related to their life-cycle. They reproduce at species-specific depth relative to the pycnocline, and distinct temperature and salinity conditions; thus they require a water column at certain depths for ontogenetic vertical migration and reproduction [51,52]. Simple morphologies (r-strategists) which are the most cosmopolitan and opportunistic taxa, inhabit shallow, more nutrient-rich, eutrophic waters [53,54]. Planktonic foraminifera in the upper Badenian part of succession include *Globigerina* (with *Globigerina bulloides* being dominant within this group) and rarely recorded *Trilobatus* and *Velapertina*. *Globigerina bulloides* reproduces primarily within the upper 60 m of the water column and exhibits maximum abundance at this depth [49,52,55,56]. It is also considered to be an indicator of cooler [57,58] and nutrient-rich, eutrophic waters [53,59–61].

The ratio between planktonic and benthic foraminifera (P/B) is related to water depth and the percentage of planktonic foraminifera generally increases with increasing distance from the shore. However, next to water depth the oxygen level of bottom waters has a profound effect on the

abundance of benthic foraminifera. This significantly influences the percentage of planktonic foraminifera in assemblages [41]. According to foraminiferal TROX model [62] benthic foraminifera distribution is a function of the interplay between food availability and oxygen concentrations. The dominance of infaunal species is interpreted as an indicator of an increase of organic matter supply and dominance of the eutrophic and dysoxic environments. In oligotrophic and well-oxygenated environments, assemblages are dominated by epifaunal species. The variations in the proportion of epifaunal and infaunal species indicate distinctive inputs of organic matter (phytodetritus input *versus* bacterial activity, respectively) [63]. The dominance of infaunal species, mainly buliminids and uvigerinids throughout the upper Badenian part of the studied interval (samples 8 to 25) indicates increased supply of organic matter to the sea floor, dominance of eutrophic conditions and impoverishment of bottom waters in oxygen in this area. Twice in the studied interval benthic foraminifera were not recorded: in sample 10 and 29. Their absence can be explained by short term anoxia at the bottom of the sea. The alternation of assemblages dominated by infaunal *Bulimina*, *Uvigerina*, *Angulogerina* and in lesser degree by *Bolivina* may be a result of a slightly different requirements of a type of food or oxygen level of each taxon. In the uppermost Badenian (samples 27 and 28) contribution of infaunal taxa decreases and diversity increases what suggest mesotrophic conditions in surface waters and oxygenation increase of bottom water.

There is also one more factor which could influence composition of benthic foraminiferal assemblages. Middle Miocene tectonic activity in the Carpathian Foredeep [64] resulted in intensive volcanism with enhanced input of volcanoclastic material [3,65]. Studies and monitoring of changes in composition of benthic foraminiferal assemblages from the South China Sea following the 1991 Mt Pinatubo ash fall documented the great impact of a few cm thick ash layer on foraminiferal association [66,67].

The Badenian/Sarmatian boundary as correlated with a sudden extinction of stenohaline foraminifera (BSEE) is placed just above the sample 28 (within the lowermost part of the *Syndesmya* Beds). The overlying sample 29 is almost barren of foraminifera, of both groups planktonic and benthic ones. Higher up in the section, the assemblage VII dominated by elphidiids alternates with the assemblage VIII dominated by miliolids. These groups of foraminifera are euryhaline and can tolerate a wide range of salinity: from brackish to elevated. Keeled species of *Elphidium* prefer inner shelf environments characterized by salinity 30-70‰ and 0-50 water depth. Unkeeled species occur in brackish-hypersaline marshes and lagoons showing salinity range of 0-70‰ [33]. Miliolids (*Quinqueloculina*, *Triloculina*) occur in marine-hypersaline (salinity 32 to 55-65‰), mainly hypersaline lagoons or marine inner shelf [33]. Replacement of stenohaline foraminiferal assemblages by euryhaline ones indicates a salinity increase while the disappearance of planktonic foraminifera suggests a shallowing of the sea.

The next almost monospecific assemblage (assemblage IX) that is dominated by *Anomalinoidea dividens* probably reflects a salinity lowering to normal marine values, although [68] suggested that the occurrence of this taxon in the palaeoenvironmental setting characterized by stratified water column which suppressed most of the benthic life and stimulated the faunas in the upper, well oxygenated, water body may have resulted from the planktonic or pseudo-planktonic mode of life.

The presence of marine palynomorphs (dinoflagellate cysts and foraminiferal organic linings) suggests that most of the studied section accumulated in marine environments. However, changes in palynofacies and the composition of aquatic palynomorph assemblages among particular samples suggests that these environmental conditions were unstable, while being subjected to numerous changes at varying scales. These changes include sea-level fluctuations, salinity, and climatic changes. All of these factors may have played important roles in the aforementioned changes in aquatic assemblages.

Undoubtedly, the lower part of the studied borehole interval (samples 8–28; the *Pecten* Beds and the lowermost part of the *Syndesmya* Beds) accumulated in a marine environment influenced by neighbouring land. The upward-decreasing proportions of cuticles suggest that land influences were gradually decreasing; the simultaneous increase in pollen grains (Figure 8) confirms this interpretation, as most of the grains were bisaccate forms, which are studied, can become airborne,

and can be transported for long distances (the so-called Neves effect; see, e.g., [69,70]). However, there were no other signs of land influences, such as a salinity decrease; there were neither freshwater algae nor dinoflagellate cysts that prefer low-salinity waters. Despite the relatively intense land influence, this interval was presumably deposited under relatively offshore conditions compared with the interval above sample 28. Only this interval yielded *Impagidinium* and *Nematosphaeropsis*, two dinoflagellate cyst genera commonly associated with offshore waters (e.g., [71–73]), while the upper interval yielded only a single *Impagidinium* only (sample 49; Table 2).

The interval below the Badenian/Sarmatian boundary (samples 17–28) showed a series of environmental fluctuations manifested by alternating changes in aquatic palynomorph compositions. High-diversity marine palynomorph assemblages dominated by *Spiniferites* alternated with less diverse *Batiacasphaera*-dominated assemblages. Moreover, *Nematosphaeropsis labyrinthus* occurred during this interval and exhibited a negative correlation with *Batiacasphaera* (Figure 9).

*Spiniferites* (mainly *S. ramosus* and the morphologically similar *Achomosphaera*) occurs in a broad marine environment spectrum and is commonly treated as a cosmopolitan taxon (e.g., [71]). But, several authors, such as [74] and [75], have suggested that its frequency increases offshore. It is also present in the marine Middle Miocene strata of the Carpathian Foredeep and is most frequent in marine shelf environments (e.g., [76]). This suggests that the samples that yielded diversified assemblages (with frequent *Spiniferites*) represents strata accumulated in a marine environment, representing an offshore setting, in contrast to those that yielded impoverished assemblages with common *Batiacasphaera*. Although the latter genus was described by [77] (*Batiacasphaera micropapillata* Complex including *B. micropapillata* and *B. minuta*) as typical for outer neritic to oceanic waters with slightly increased salinity, *Batiacasphaera* (mainly *B. sphaerica*) tends to exhibit increased frequencies in restricted environments possibly associated with water shallowness and/or increased salinity [76,78]. The negative correlation between *Batiacasphaera* and *Nematosphaeropsis labyrinthus* may be an additional clue suggesting sea-level fluctuations during this period. However, *Nematosphaeropsis labyrinthus* is treated as a cold-water species (e.g., [79]) in contrast to *Batiacasphaera*, which is believed to be a temperate-to-warm-water taxon [77]. This suggests that an acme of *N. labyrinthus* just below the Badenian/Sarmatian boundary may be the result of a temperature drop in sea-surface waters (a similar inverse correlation between *N. labyrinthus* and *Batiacasphaera micropapillata* was noted by [80], and interpreted as a possible cooling). Notably high frequencies of *N. labyrinthus* were found in the Pecten Beds overlying the Badenian evaporites in the Carpathian Foredeep [81]. This might indicate a cooling period (or periods) after accumulation of the evaporitic series. However, *N. labyrinthus* is known from warm-water middle Badenian Korytnica Clays and their offshore age equivalents – the Skawina Beds [76,78].

The interval that occurred just above (samples 29 and 31) was characterized by a lack of dinoflagellate cysts and flowering of Leiosphaeridiaceae. It could be any of the aforementioned environmental factors – albeit of a larger magnitude – the one that led to such a drastic environmental change in the earliest Sarmatian associated with a collapse of dinoflagellate floras. The precise reconstruction of environmental changes during the accumulation of these strata is difficult. The absence of dinoflagellate cysts (Figure 8) indicated disastrous conditions for dinoflagellate cysts. However, the most likely reason was that salinity increased above the tolerable level, even for hypersaline forms (e.g., *Polysphaeridium*), but was still favourable for *Leiosphaeridia*. This prasinophyta genus (e.g., [82]) was described from the Carpathian Foredeep, more specifically from middle Badenian evaporitic strata accumulated during increased water salinity conditions (e.g., [78]), and upper Badenian stress deposits [83]. These possible hypersaline conditions were associated with stagnant, possibly stratified waters that led to anoxic conditions in the bottom waters, as evidenced by AOM (Figure 8).

The cessation of these conditions was caused by a possible sea-level rise and the gradual return of a less saline water regime. The latter interpretation is supported by the fact that sample 33 yielded a high frequency of *Polysphaeridium* (a genus known from hypersaline environments, e.g., [84]), which benefited from the transitional salinity levels between the highly saline conditions that were disastrous for the genus (samples 29 and 31) and the conditions that prevailed during the

accumulation of the higher interval (samples 35 and above). *Polysphaeridium* was described from a similar position, i.e., from the strata directly overlying the chemical deposits in other areas of the Miocene of the Carpathian Foredeep (e.g., [83,85–87]).

The higher interval (samples 35–55, i.e., the upper part of the *Syndesmya* Beds and the overlying part of the Krakowiec Clays: Figure 9) was deposited under more restricted and variable environmental conditions (compared to those of the basal interval, namely samples 8–28).

This interval yielded no offshore species (except for a single *Impagidinium* specimen in sample 49), and the diversity and number of taxa decreased significantly (Figure 9). However, the factors responsible for these conditions remain unclear. There were no clear indicators of sea-level or salinity changes. An important event was the disappearance of *Batiacasphaera*, which can be interpreted either as a result of cooling or changes in sea-water chemistry; however, its nature remains uncertain. A drop in sea-surface water temperature is also suggested by the lack of *Nannobarbophora gedlii*, which is believed to be a warm-water species [88].

Some recorded events may indicate fluctuations in the salinity level. There are almost no stenohaline foraminiferal organic linings (present in the lower interval, namely samples 8–28), and some taxa known to benefit from low-salinity, commonly nutrient-rich waters, show temporarily enriched frequencies (e.g., [73]). These include *Lingulodinium machaerophorum* and heterotrophic Congruentidiaceae (peridinioids are represented in the present material by *Selenopemphix* and *Lejeunecysta*). *L. machaerophorum* dominated sample 39, whereas rare peridinioids occurred in the top interval (samples 39–55), forming an acme of *Selenopemphix* in sample 41 (Table 2; Figure 9). This interval, in turn, was preceded by samples 33 and 37, which yielded *Polysphaeridium* – a hypersaline taxon (see above). Another characteristic feature of the strata above the *Syndesmya* Beds was the common occurrence of *Systematophora*. This genus was missing or rarely exceeded 10% in the lower interval, whereas it accounted for over 40%, maximally over 60%, in some samples from the upper interval (Figure 9). However, palaeoenvironmental preferences of *Systematophora* are poorly understood. [75] included *Systematophora placacantha* in the *Glaphyrocysta* eco-group, which included open-marine (i.e., fully marine) and warm-water taxa. [71] highlighted the widespread occurrence of this genus and linked it to shelf environments in any climatic setting. Analysis of *Systematophora* (*S. placacantha* and *S. ancyrea*) occurrences in the Miocene of the Carpathian Foredeep shows a broad environmental tolerance range of this genus, as it is a member of fully marine (e.g., [76,89]) and impoverished assemblages (e.g., [81]). However, a noticeable feature of the occurrence of this genus is the remarkable frequency increase in Sarmatian deposits (e.g., [81]), which may be linked to the euryhaline nature of this genus. A similar acme of *Systematophora* (as *Clesitosphaeridium*) was noted in the uppermost Badenian–lower Sarmatian Paratethyan deposits in Hungary [90].

Another clue suggestive of fluctuating, mainly restricted environments during the accumulation of the upper part of the *Syndesmya* Beds and the Krakowiec Clay is the persistent presence of *Leiosphaeridia* (and presumably some other sphaeromorphic, smooth acritarchs). Their occurrence may reflect either salinity fluctuations (see above), but also generally cooler surface waters and/or increased nutrient availability (see [80], p. 55 and references therein).

An exception was an assemblage yielded from sample 51, i.e., a low-diversity assemblage dominated by *Batiacasphaera*, with no peridinioids. Its palynofacies is also exceptional as it includes no AOM in contrast to the remaining samples from this interval. The appearance of *Batiacasphaera* may be related to the temporal return of fully marine conditions, possibly due to a short-term sea-level rise. The AOM that occurred in most of the samples from this interval indicates stagnant waters with a low oxygen contents in the bottom environments. Even a low-magnitude sea-level rise could induce sea-water circulation and better ventilation at the bottom. The appearance of *Batiacasphaera* in sample 51 may also reflect an increase in surface sea water temperature.

#### 4.2. Plant communities and terrestrial palaeoenvironment

Although some sporomorphs are corroded, palynological analysis provided valuable information about palaeovegetation, palaeogeography, and palaeoclimate. The degree of pollen grain destruction can be also used as a source of information. For example, some bisaccate

pollen grains were heavily corroded, particularly in samples with high marine palynomorph contents (lower part of the section; Figure 10). This pollen could have easily been transported over long distances, from both the northern sea shores and the Carpathians, and their abundance tends to increase offshore (the so-called Neves effect). Nevertheless, conifers likely played an important role in the coastal forests. For example, the better-preserved non-bisaccate pollen grains of *Tsuga* and *Sciadopitys* were the most likely components of mesophytic forests in the vicinity. In the upper section of the profile (above sample 27) some pollen grains were found in clumps (*Ericaceae*, *Fagus*, and *Salix*), which may also indicate the proximity of their habitats to the coast.

The results of the palynological analysis revealed the presence of mesophytic and wetland vegetation along shoreline of Paratethys during sedimentation. Mesophytic forests were composed of *Fagus*, *Quercus* (also thermophilous oaks producing pollen of the fossil-species *Quercoidites henricii*), *Tsuga* and other conifers, *Carpinus*, *Tilioideae*, and others, with a relatively small admixture of *Castaneoideae* and other thermophilous taxa. *Ulmus*, *Pterocarya*, *Carya*, *Zelkova*, *Liquidambar*, *Alnus*, *Acer*, *Fraxinus*, and *Salix* probably grew in riparian forests in periodically flooded areas, such as river valleys. *Taxodium* and/or *Glyptostrobus*, together with *Alnus* and *Nyssa*, were likely elements of swamp forests, growing in permanently flooded areas in the vicinity. Similarly, *Osmunda* and other ferns grew in wet places. Various shrubs of the *Ericaceae* family as well as *Myrica* and *Ilex*, probably were components of shrub communities. The abundance of ericaceous plants may be related to open areas adjacent to the coastline, within coastal peat-bogs or heathland-type shrub vegetation and partly with forest undergrowth [91,92]. Herbs were represented mainly by the *Cyperaceae*, *Sparganiaceae*/*Typhaceae*, and *Poaceae* families, and at least some of them could have grown in freshwater margins (e.g., *Cyperaceae*, *Sparganium* and/or *Typha*). The presence of numerous pollen grains of *Chenopodiaceae* coincides with the occurrence of high-salinity habitats, such as seashores, because many of the recent species of this family are halophytes that tolerate salty soils.

The changes in the frequency of the spore-pollen taxa were rather small, and no rapid change in vegetation was observed. Nevertheless, the lower section appeared richer in palaeotropical taxa (*Ilexpollenites margaritatus*, *Symplocoipollenites vestibulum*, and *Tricolporopollenites indeterminatus*), although it generally had a high content of marine palynomorphs, and the land elements have had little chance of reaching this location. In contrast, the upper section contained more diverse *Pinaceae* pollen grains, including *Abies* and *Picea*, which can be interpreted as a manifestation of the mountain forest development. Such changes are gradual and modified by the changing sea influences; therefore, a boundary between the levels cannot be set.

Diverse fungal microremains (i.a. *Asterosporium*, *Cephalothecoidomyces*, *Diporothea*, *Phragmothyrites*, *Potamomyces*, and cf. *Tetraploa*) were found, mainly in the upper part of the profile. Their presence indicated a brackish environment and their proximity to the sea-shore. *Cephalothecoidomyces* G. Worobiec, Neumann & E. Worobiec and *Potamomyces* K.D. Hyde suggest that abundant decaying wood could have accumulated in humid and swampy places [93–95]. Contemporary *Diporothea webbiae* D. Hawksworth, B. van Geel & P. Wiltshire, similar to the fossil specimen from Babczyn, is associated with alder carrs [96]. Therefore, it is probable that the coastal areas, at least in some parts, were overgrown by swamp forests, as also indicated by the fossil pollen grains studied. The co-occurrence of the fossil conidia of the *Asterosporium asterospermum* (Pers.) Hughes fungus with *Fagus* pollen grains indicates that the beech trees grew close to the seashore [97].

The results of the palynological analysis indicated that the climate during the deposition of the sediments was generally warm temperate, warmer than the present-day climate of Poland), mild (without severe winters), and rather humid. Some fungal taxa (notably *Potamomyces* and probably *Tetraploa*) indicated a humid and warm, subtropical climate during this period [93,95,98].

Miocene sediments in Poland have relatively rich palynological documentation, but most studies come from the Polish Lowlands [99,100]. In contrast, palynological (spore-pollen) studies of the Carpathian Foredeep are rare. Moreover, Badenian–Sarmatian marine sediments that were previously analysed were mainly from the western, Silesian region of the Carpathian Foredeep [99,101–104]. In addition, palynofloras from several boreholes in the Bochnia and Wieliczka regions [105], including borehole Kłaj 1 [106] as well as from the sulphur deposits at Piaseczno near

Tarnobrzeg [91], were studied. Although the frequency of sporomorphs in these deposits were usually low, the samples had usually similar compositions, exhibiting abundant conifers with high levels of *Pinus* as well as *Abies*, *Tsuga* and *Picea*. Among the deciduous trees, *Quercus*, *Ulmus*, *Castanea*, *Engelhardia*, and *Fagus* played the most significant role, whereas *Carya*, *Pterocarya*, and *Tricolporopollenites pseudocingulum* (in some cases identified as *Rhus*) were less important. Shrubs and thermophilous ferns were also relatively frequent. Swampy plants, which are characteristic of continental sediments in the Polish Lowlands, were rare (except for *Taxodium/Glyptostrobus*), and included only taxa, such as *Alnus*, *Liquidambar*, *Myrica* and *Ilex* [92].

The Babczyn palynoflora is very similar to the spore-pollen assemblage from the Jamnica S-119 borehole [92] drilled in the upper Badenian and lower Sarmatian marine deposits near Tarnobrzeg in the northeastern part of the Carpathian Foredeep. The Jamnica palynoflora was dominated by coniferous trees, especially *Pinus*, as well as *Taxodium/Glyptostrobus* (identified as Taxodiaceae–Cupressaceae), *Tsuga*, *Abies*, *Picea*, *Cedrus*, and *Sciadopitys*, whereas the pollen of *Sequoia* was identified only in some samples. Among deciduous trees and shrubs *Ulmus*, *Quercus*, *Alnus*, *Carya*, *Fagus*, Ericaceae, *Engelhardia*, *Pterocarya*, and *Quercoidites henricii* were the most frequent. Some samples frequently contained small percentages of tree and shrub taxa such as *Betula*, *Carpinus*, *Liquidambar*, *Salix*, *Acer*, *Castanea*, *Fraxinus*, *Juglans*, *Nyssa*, *Parrotia*, *Myrica*, *Symplocos*, Cyrillaceae/Clethraceae, *Ilex*, *Tricolporopollenites pseudocingulum*, and others. Pollen grains of herbaceous plants were very rare, with sporadic Chenopodiaceae, Cyperaceae, Poaceae, Lamiaceae, and *Nuphar*. Similarly, the spores of ferns (Polypodiaceae, *Osmunda* and Cyatheaceae-Schizaeaceae) and *Sphagnum* appeared in very small quantities. The composition of plant communities in the entire Jamnica section was quite homogeneous and no temporal flora changes were observed. The highest content of pollen material in the middle part of the Jamnica profile, with more abundant pollen from deciduous trees and herbaceous plants, accompanied by a simultaneous decrease in *Pinus*, indicated a more landward position of that part of the profile. Differences in the pollen spectra from Jamnica may suggest rather a shoreline migration at this level than changes of palaeovegetation caused by climate [92].

[107] made similar assumptions for the entire Carpathian Region. Their palaeofloristic and palaeoclimatic reconstructions showed that the upper Badenian and lower Sarmatian floras were closer to each other than to the flora of the previous and subsequent stages. The evolutionary process during the late Badenian–early Sarmatian continued the main trends of forest floral and vegetational evolution, stimulated by the gradual cooling of the climate [108]. At this time the replacement of the subtropical forest communities by warm temperate and temperate forest communities was observed in the Central Paratethys. In the south-eastern part of Ukraine (Eastern Paratethys) temperate forests were replaced by herb communities. This process was evident in all studied sections, albeit involving spatial differences [107,109,110].

#### 4.3. Implications

Although a consensus exists that at the Badenian-Sarmatian boundary a major change in the benthic and planktonic foraminiferal assemblages in the Central Paratethys occurred (e.g., [111]), there are various hypotheses regarding its drivers. [112] concluded that this change occurred within a time interval of less than 10 kyr and it was related to a change in the configuration of the Central–Eastern Paratethys gateway (Barlad Strait). It could have been also related to a minor rise in global sea level that otherwise affected the Sarmatian transgression in many other basins of the Central Paratethys ([113], with references therein). [114] suggested a continuous sea level rise in the Eastern Paratethys due to fresh-water input by rivers and thus the Sarmatian transgression event could have resulted from a full connection between the both Paratethyan basins. It was repeatedly suggested that the transgression was accompanied by a drastic change in water chemistry exemplified by a supposed change from marine to brackish conditions in the Central Paratethys (cf. [26,115]) what otherwise could be expected considering the inflow of Eastern Paratethyan water to the Central Paratethys. Our data do not support the brackish-water environments at the onset of the Sarmatian. Instead, the domination of the foraminiferal assemblages above the Badenian/Sarmatian boundary

by miliolids, what is commonly observed in various parts of the Carpathian Foredeep Basin in Poland [8,14,116], implies normal to hypersalinity conditions lower than 50 psu [33,117]. Such a conclusion is also supported by the palynological data reported in this paper. [118] concluded that the fully marine to hypersaline conditions existed in the late Sarmatian, and our result suggest that this conclusion is also valid for early Sarmatian.

## 5. Conclusions

Qualitative and quantitative analyses of foraminifera and the aquatic palynomorphs in the Badenian-Sarmatian strata of the Babczyn 2 borehole, one of the key sections in SE Poland, showed that the studied interval accumulated under variable, unstable sedimentary conditions in marine environments.

The dominance of infaunal species, mainly buliminids and uvigerinids throughout the upper Badenian part of the studied interval (samples 8 to 25) indicates mostly suboxic conditions. For the uppermost Badenian mesotrophic conditions in surface waters and oxygenation increase of bottom water is concluded. The Badenian/Sarmatian boundary as correlated with a sudden extinction of stenohaline foraminifera is placed just above the sample 28 (within the lowermost part of the *Syndesmya* Beds). The overlying sample 29 is almost barren of planktonic and benthic foraminifera, and the lack of benthic forms may be explained by short term anoxia at the bottom of the sea. Euryhaline early Sarmatian benthic foraminiferal assemblages indicate a salinity increase while the lack of planktonic foraminifera suggests a shallowing of the sea.

An acme of *N. labyrinthus* just below the Badenian/Sarmatian boundary may be the result of a temperature drop in sea-surface waters. The interval that occurred just above (samples 29 and 31) was characterized by a lack of dinoflagellate cysts and flowering of Leiosphaeridiaceae suggesting hypersaline conditions which were associated with stagnant, possibly stratified waters that led to anoxic conditions in the bottom waters, as evidenced by AOM. The subsequent cessation of these hypersaline conditions was caused by a possible sea-level rise and the gradual return of a less saline water regime. The higher interval (samples 35–55) was deposited under more restricted and variable environmental conditions including brackish environment as indicated by diverse fungal microremains found in the upper part of the profile.

The results of the spore-pollen analysis revealed the presence of mesophytic and wetland vegetation along shoreline of Paratethys during sedimentation and indicated that the climate during the deposition of the sediments was generally warm-temperate, mild, and rather humid.

**Author Contributions:** Conceptualization, D.P. and T.P.; methodology, D.P., P.G., E.W. and G.W.; validation, D.P., P.G., E.W. and G.W.; formal analysis, D.P., P.G., E.W., G.W. and T.P.; investigation, D.P., P.G., E.W., G.W. and T.P.; resources, D.P.; data curation, D.P., P.G., E.W. and G.W.; writing—original draft preparation, D.P., P.G., E.W., G.W. and T.P.; writing—review and editing, T.P., P.G., D.P., E.W. and G.W.; visualization, D.P., P.G., E.W., G.W. and T.P.; supervision, D.P.; project administration, D.P.; funding acquisition, D.P. All authors have read and agreed to the published version of the manuscript.

**Funding:** This research was funded by the National Science Centre, Poland, grant number UMO-2017/27/B/ST10/01129.

**Data Availability Statement:** The data presented in this study are available on request.

**Conflicts of Interest:** The authors declare no conflicts of interest. The funders had no role in the design of the study; in the collection, analyses, or interpretation of data; in the writing of the manuscript; or in the decision to publish the results.

## References

1. Laskarev, V. Sur les equivalentes du Sarmatien supérieur en Serbie. In: *Recueil de travaux offert a M. Jovan Cvijic par ses amis et collaborateurs*; Vujević, P., Ed.; Državna Štamparija, Beograd, **1924**; pp. 73-85.
2. Harzhauser, M., Piller, W.E. Benchmark data of a changing sea — palaeogeography, palaeobiogeography and events in the Central Paratethys during the Miocene. *Palaeogeogr. Palaeoclimatol. Palaeoecol.* **2007**, *253*, 8-31.

3. Śliwiński, M., Bąbel, M., Nejbert, K., Olszewska-Nejbert, D., Gąsiewicz, A., Schreiber, B.C., Be-Nowitz, J.A., Layer, P. Badenian–Sarmatian chronostratigraphy in the Polish Carpathian Foredeep. *Palaeogeogr. Palaeoclimatol. Palaeoecol.* **2012**, 326–328, 12–29.
4. Palcu, D.V., Kouwenhoven, T.J., Krijgsman, W. Reply to “Comment on the Badenian-Sarmatian extinction event in the Carpathian foredeep basin of Romania: Paleogeographic changes in the Paratethys (Palcu et al., 2015)” by Silye and Filipescu (2016). *Glob. Planet. Change* **2016**, 145, 141–142.
5. Silye, L., Filipescu, S. Comment on “The Badenian-Sarmatian Extinction Event in the Carpathian foredeep basin of Romania: Paleogeographic changes in the Paratethys domain” (Palcu et al., 2015). *Glob. Planet. Change* **2016**, 145, 17–19.
6. Peryt, T.M., Kasprzyk, A. Carbonate-evaporite sedimentary transitions in the Badenian (middle Miocene) basin of southern Poland. *Sediment. Geol.* **1992**, 76, 257–271.
7. Peryt, D., Gedl, P., Peryt, T.M. Marine transgression(s) to evaporite basin: The case of middle Miocene (Badenian) gypsum in the Central Paratethys, SE Poland. *Jour. Palaeogeogr.* **2020**, 9, 16.
8. Peryt, D., Garecka, M., Peryt, T.M. Foraminiferal and calcareous nannoplankton biostratigraphy of the upper Badenian–lower Sarmatian strata in the SE Polish Carpathian Foredeep. *Geol. Quart.* **2021**, 65, 18.
9. Łuczowska, E. Foraminiferal zones in the Miocene, south of the Holy Cross Mts. *Bull. Acad. Pol. Sci., Sér. Sci. Géol. Géogr.* **1963**, 11, 29–34.
10. Łuczowska, E. The micropaleontological stratigraphy of the Miocene in the region of Tarnobrzeg-Chmielnik (in Polish with English summary). *Pr. Geol.* **1964**, 20, 1–72.
11. Łuczowska, E. A new zone with *Praeorbulina indigena* (Foraminifera, Globigerinidae) in the Upper Badenian (Tortonian s.s.) of Central Paratethys. *Roczn. Polsk. Tow. Geol.* **1971**, 40, 445–448.
12. Odrzywolska-Bieńkowska, E. Micropaleontological stratigraphy of the Miocene of central part of the Carpathian Foredeep (in Polish with English summary). *Prz. Geol.* **1975**, 23, 597–603.
13. Czepiec, I. Biostratigraphy and paleoenvironment of Sarmatian marginal zone of Poland (in Polish with English summary). *Kwart. AGH, Geologia* **1996**, 22, 309–338.
14. Kirchner, Z. Miocene stratigraphy of the Central Carpathian Foreland based on microfaunal studies (in Polish with English summary). *Acta Geol. Pol.* **1956**, 6, 421–450.
15. Cicha, I., Rögl, F., Rupp, Ch., Čtyroká, J. (eds.). Oligocene-Miocene foraminifera of the Central Paratethys. *Abh. Senckenberg. Naturforsch. Ges.* **1998**, 549, 1–325.
16. Filipescu, S. *Anomalinoidea dividens* bioevent at the Badenian/Sarmatian boundary – a response to paleogeographic and paleoenvironmental changes. *Studia Univ. Babeş-Bolyai, Geologia* **2004**, 49 (2), 21–26.
17. Dumitriu, S.D., Loghin, S., Dubicka, Z., Melinte-Dobrinescu, M.C., Paruch-Kulczycka, J., Ionesi, V. Foraminiferal, ostracod, and calcareous nannofossil biostratigraphy of the latest Badenian – Sarmatian interval (Middle Miocene, Paratethys) from Poland, Romania and the Republic of Moldova. *Geol. Carpath.* **2017**, 68, 419–444.
18. Ney, R., Burzewski, W., Bachleda, T., Górecki, W., Jakóbczak, K., Słupczyński, K. Outline of paleogeography and evolution of lithology and facies of Neogene layers on the Carpathian Foredeep (in Polish with English summary). *Prace Geol.* **1974**, 82, 3–65.
19. Dziadzio, P., Maksym, A., Olszewska, B. Miocene deposition in the eastern part of the Carpathian Foredeep in Poland (in Polish with English summary). *Prz. Geol.* **2006**, 54, 413–420.
20. Alexandrowicz, S.W., Garlicki, A., Rutkowski, J. Podstawowe jednostki litostratygraficzne miocenu zapadliska przedkarpaccyjskiego (in Polish). *Kwart. Geol.* **1982**, 26, 470–471.
21. Peryt, T.M. The beginning, development and termination of the Middle Miocene Badenian salinity crisis in Central Paratethys. *Sediment. Geol.* **2006**, 188–189, 379–396.
22. de Leeuw, A., Tulbure, M., Kuiper, K.F., Melinte-Dobrinescu, M.C., Stoica, M., Krijgsman, W. New <sup>40</sup>Ar/<sup>39</sup>Ar, magnetostratigraphic and biostratigraphic constraints on the termination of the Badenian Salinity Crisis: Indications for tectonic improvement of basin interconnectivity in Southern Europe. *Glob. Planet. Change* **2018**, 169, 1–15.
23. Pawłowska, K., Kubica, B. *Karta otworu wiertniczego Babczyn-2* (in Polish; unpublished). Archive CUG, Warszawa, **1960**.
24. Jasionowski, M., Peryt, T.M. Historia badań. In: *Budowa geologiczna Polski, tom I. Stratygrafia, część 3a Kenozoik Paleogen Neogen*, Peryt, T.M., Piwocki, M., Eds.; Polish Geological Institute, **2004**; pp. 203–212.
25. Czapowski, G. Wschodnia część zapadliska. In: *Budowa geologiczna Polski, tom I. Stratygrafia, część 3a Kenozoik Paleogen Neogen*, Peryt, T.M., Piwocki, M., Eds.; Polish Geological Institute, **2004**; pp. 239–245.
26. Palcu, D.V., Golovina, L.A., Vernyhorova, Y.V., Popov, S.V., Krijgsman, W. Middle Miocene paleoenvironmental crises in Central Eurasia caused by changes in marine gateway configuration. *Glob. Planet. Chang.* **2017**, 158, 57–71.
27. Odrzywolska-Bieńkowska, E. Porównanie wybranych głębszych profile mikrofaunistycznych rejonu świętokrzyskiego i lubelskiego (in Polish). *Sprawozd. Posiedz. Kom. Nauk. PAN, Kraków* **1972**, 16, 493–494.
28. Van der Zwaan, G.J. Paleoecology of late Miocene Mediterranean Foraminifera. *Utrecht Micropaleont. Bull.* **1982**, 25.

29. Culver, S. New foraminiferal depth zonation of the northwestern Gulf of Mexico. *Palaios* **1988**, *3*, 69–85.
30. Lutze, G.F., Thiel H. Epibenthic foraminifera from elevated microhabitats; *Cibicoides wuellerstorfi* and *Planulina ariminensis*. *Jour. Foram. Res.* **1989**, *19*, 153–158.
31. Verhallen, P. Late Pliocene to early Pleistocene Mediterranean mud-dwelling foraminifera; influence of a changing environment on community structure and evolution. *Utrecht Micropaleont. Bull.* **1991**, *40*, 1–219.
32. Murray, J.W. *Ecology and Palaeoecology of Benthic Foraminifera*. Longman, Avon, **1991**; pp. 408.
33. Murray, J.W. *Ecology and Applications of Benthic Foraminifera*. Cambridge University Press, Cambridge, **2006**; pp. 426.
34. Sjoerdsma, P.G., van der Zwaan, G.J. Simulating the effect of changing oceanic flux and oxygen content on the distribution of benthic foraminifers. *Marine Micropaleont.* **1992**, *19*, 163–180.
35. Goner, M. Foraminiferida and palaeoenvironment of the Badenian Formations (Middle Miocene) in Upper Silesia (Poland) (in Polish with English summary) (in Polish with English summary). *Stud. Natur.* **2001**, *48*, 1–211.
36. Hohenegger, J. Estimation of environmental paleogradient values based on presence/absence data: a case study using benthic foraminifera for paleodepth estimation. *Palaeogeogr. Palaeoclimatol. Palaeoecol.* **2005**, *217*, 115–130.
37. Kouwenhoven, T.J., van der Zwaan, G.J. A reconstruction of late Miocene Mediterranean circulation patterns using benthic foraminifera. *Palaeogeogr. Palaeoclimatol. Palaeoecol.* **2006**, *238*, 373–385.
38. Kaminski, M.A. Calibration of the Benthic Foraminiferal Oxygen Index in the Marmara Sea. *Geol. Quart.* **2012**, *56*, 757–764.
39. Dumitriu, S.D., Dubicka, Z., Loghin, S., Melinte-Dobrinescu, M.C., Paruch-Kulczycka, J. The evolution of the Carpathian Foredeep Basin during the latest Badenian and Sarmatian (Middle Miocene): inferences from micropalaeontological data. *Geol. Quart.* **2020**, *64*, 1004–1022.
40. Van der Zwaan, G.J., Duijnste, I.A.P., den Dulk, M., Ernst, S.R., Jannink, N.T., Kouwenhoven, T.J. Benthic foraminifers: proxies or problems? A review of paleoecological concepts. *Earth-Sci. Rev.* **1999**, *46*, 213–236.
41. Van Hinsbergen, D.J.J., Kouwenhoven, T.J., van der Zwaan, G.J. Paleobathymetry in the backstripping procedure: correction for oxygenation effects on depth estimates. *Palaeogeogr. Palaeoclimatol. Palaeoecol.* **2005**, *221*, 245–265.
42. Holcová, K., Zágorský, K. Bryozoa, foraminifera and calcareous nannoplankton as environmental proxies of the "bryozoan event" in the Middle Miocene of the Central Paratethys (Czech Republic). *Palaeogeogr. Palaeoclimatol. Palaeoecol.* **2008**, *267*, 216–234.
43. Hart, M.B., Fisher, J.K., Smart, C.W., Speers, R., Wall-Palmer, D. Re-colonization of hostile environments by benthic foraminifera: an example from Montserrat, Lesser Antilles Volcanic Arc. *Micropaleont.* **2022**, *69*, 1–27.
44. Stuchlik, L., Ziemińska-Tworzydło, M., Kohlman-Adamska, A., Grabowska, I., Ważyńska, H., Słodkowska, B., Sadowska, A. *Atlas of pollen and spores of the Polish Neogene. Vol. 1 – Spores*; W. Szafer Institute of Botany, Polish Academy of Sciences, Kraków, **2001**; 158 pp.
45. Stuchlik, L., Ziemińska-Tworzydło, M., Kohlman-Adamska, A., Grabowska, I., Ważyńska, H., Sadowska, A. *Atlas of pollen and spores of the Polish Neogene. Vol. 2 – Gymnosperms*; W. Szafer Institute of Botany, Polish Academy of Sciences, Kraków, **2002**; 237 pp.
46. Stuchlik, L., Ziemińska-Tworzydło, M., Kohlman-Adamska, A., Grabowska, I., Słodkowska, B., Ważyńska, H., Sadowska, A. *Atlas of pollen and spores of the Polish Neogene. Vol. 3 – Angiosperms (1)*; W. Szafer Institute of Botany, Polish Academy of Sciences, Kraków, **2009**; 233 pp.
47. Stuchlik, L., Ziemińska-Tworzydło, M., Kohlman-Adamska, A., Grabowska, I., Słodkowska, B., Worobiec, E., Durska, E. *Atlas of pollen and spores of the Polish Neogene. Vol. 4 – Angiosperms (2)*; W. Szafer Institute of Botany, Polish Academy of Sciences, Kraków, **2014**; 466 pp.
48. Nalepka, D., Walanus, A. Data processing in pollen analysis. *Acta Palaeobot.* **2003**, *43*, 125–134.
49. Hemleben, C., Spindler, M., Anderson, O.R. *Modern Planktonic Foraminifera*; Springer, New York, **1989**; 363 pp.
50. Schiebel, R., Bijma, J., Hemleben, C. Population dynamics of the planktic foraminifer *Globigerina bulloides* from the eastern North Atlantic. *Deep-Sea Res. I* **1997**, *44*, 1701–1713.
51. Caron, M. Cretaceous planktic foraminifera. In: *Plankton Stratigraphy*; Bolli, H.M., Saunders, J.B., Perch-Nielsen, K., Eds.; Cambridge University Press, **1985**; pp. 17–86.
52. Schiebel, R., Hemleben, C. Modern planktonic foraminifera. *Paläont. Zt.* **2005**, *79*, 135–148.
53. Hebbeln, D., Marchant, M., Wefer, G. Seasonal variations of the particle flux in the Peru-Chile Current at 30°S under normal and El Niño conditions. *Deep Sea Research Part II: Topical Studies in Oceanography* **2000**, *47*, 2101–2128.
54. Petrizzo, M.R. Palaeoceanographic and palaeoclimatic inferences from Late Cretaceous planktonic foraminiferal assemblages from the Exmouth Plateau (ODP Sites 762 and 763, eastern Indian Ocean). *Mar. Micropaleontol.* **2002**, *45*, 117–150.

55. Schiebel, R., Bijma, J., Hemleben, C. Population dynamics of the planktic foraminifer *Globigerina bulloides* from the eastern North Atlantic. *Deep Sea Res. Part I* 1997, 44, 1701-1713.
56. Di Stefano, A., Verducci, M., Lirer, F., Ferraro, L., Iaccarino, S.M., Hüsing, S.K., Hilgen, F.J. Paleoenvironmental conditions preceding the Messinian Salinity Crisis in the Central Mediterranean: integrated data from the Upper Miocene Trave section (Italy). *Palaeogeogr., Palaeoclimatol., Palaeoecol.* **2010**, 297, 37–53.
57. Bé, A.W.H., Tolderlund, D.S. Distribution and ecology of living planktonic foraminifera in surface waters of the Atlantic and Indian Oceans. In: *The Micropaleontology of Oceans*; Funnell, B.M., Riedel, W.R., Eds.; Cambridge University Press, Cambridge, **1971**; pp. 105–149.
58. Bé, A.W.H. An ecological zoogeographic and taxonomic review of recent planktonic foraminifera. In: *The Micropaleontology of Oceans*, Ramsay, A.T.S., Ed.; Academic Press, London, **1977**; pp. 1–100.
59. Thunell R., Reynolds-Sautter, L. Planktonic foraminiferal faunal and stable isotopic indices of upwelling: a sediment trap study in the San Pedro Basin, Southern California Bight. *Geol. Soc. Spec. Publ.* **1992**, 64, 77-91.
60. Schiebel, R., Hemleben, C. *Planktic Foraminifers in the Modern Ocean*. Springer, Berlin Heidelberg, **2017**; pp. 358.
61. Darling, K.F., Wade, C.M., Siccha, M., Trommer, G., Schulz, H., Abdolalipour, S., Atsushi Kurasawa, A. Genetic diversity and ecology of the planktonic foraminifers *Globigerina bulloides*, *Turborotalita quinqueloba* and *Neoglobobulimina pachyderma* off the Oman margin during the late SW Monsoon. *Mar. Micropaleont.* **2017**, 137, 64–77.
62. Jorissen, F.J., de Stigter, H.C., Widmark, J.G.V. A conceptual model explaining benthic foraminiferal microhabitats. *Mar. Micropaleont.* **1995**, 26, 3-15.
63. Rodrigues, A.R., Gómez Pivel, M.A., Schmitt, P., de Almeida, F.K., Bonetti, C. Infaunal and epifaunal benthic foraminifera species as proxies of organic matter paleofluxes in the Pelotas Basin, south-western Atlantic Ocean. *Mar. Micropaleont.* **2018**, 144, 38-49.
64. Kováč, M., Márton, E., Oszczytko, N., Vojtko, R., Hók, J., Králiková, S., Plašienka, D., Klučiar, T., Hudáčková, N., Oszczytko-Clowes, M. Neogene palaeogeography and basin evolution of the Western Carpathians, Northern Pannonian domain and adjoining areas. *Glob. Planet. Chang.* **2017**, 155, 133–154.
65. Bukowski, K., de Leeuw, A., Gonera, M., Kuiper, K.F., Krzywiec, P., Peryt, D. Badenian tuffite levels within the Carpathian orogenic front (Gdów–Bochnia area, Southern Poland): radio-isotopic dating and stratigraphic position. *Geol. Quart.* **2010**, 54, 449–464.
66. Hess, S., Kuhnt, W. Deep-sea benthic foraminiferal recolonization of the 1991 Mt Pinatubo ash layer in the South China Sea. *Mar. Micropaleont.* **1996**, 28, 171-197.
67. Hess, S., Kuhnt, W., Hill, S., Kaminski, M. A., Holbourn, A., de Leon, M. Monitoring the recolonization of the Mt Pinatubo 1991 ash layer by benthic foraminifera. *Mar. Micropaleont.* **2001**, 43, 119-142.
68. Filipescu, S. *Anomalinoidea dividens* bioevent at the Badenian/Sarmatian boundary — a response to paleogeographic and paleoenvironmental changes. *Studia Universitatis Babeş-Bolyai, Geologia* **2004**, 49, 21–26.
69. Chaloner, W.G., Muir, M. Spores and floras. In: *Coal and coal-bearing strata*; Murchison, D.G., Westoll, T.S., Eds.; Oliver and Boyd, Edinburgh, **1968**; pp. 127–146.
70. Streef, M., Richelot, C. Wind and water transport and sedimentation of miospores along two rivers subject to major floods and entering the Mediterranean Sea at Calvi (Corsica, France). In: *Sedimentation of organic particles*; Traverse, A., Ed.; Cambridge University Press, Cambridge, **1994**; pp. 59–67.
71. Brinkhuis, H. Late Eocene to Early Oligocene dinoflagellate cysts from the Priabonian type-area (northeast Italy): biostratigraphy and palaeoenvironmental interpretation. *Palaeogeogr. Palaeoclimatol. Palaeoecol.* **1994**, 107, 121–163.
72. Stover, L.E., Brinkhuis, H., Damassa, S.P., de Verteuil, L., Helby, R.J., Monteil, E., Partridge, A.D., Powell, A.J., Riding, J.B., Smelror, M., Williams, G.L. Mesozoic–Tertiary dinoflagellates, acritarchs and prasinophytes. In: *Palynology: Principles and Applications*; Jansonius, J., McGregor, D.C., Eds.; American Association of Stratigraphic Palynologists Foundation, Dallas TX, **1996**; Volume 2, pp. 641–750.
73. Sluijs, A., Pross, J., Brinkhuis, H. From greenhouse to icehouse; organic-walled dinoflagellate cysts as paleoenvironmental indicators in the Paleogene. *Earth-Sci. Rev.* **2005**, 68, 281–315.
74. Williams, G.L. Dinoflagellate cysts, their classification, biostratigraphy and palaeoecology. In: *Oceanic Micropalaeontology*, Ramsay, A.T.S., Ed.; Academic Press, London, **1977**; pp. 1231–1325.
75. Köthe, A. Paleogene dinoflagellates from northwest Germany. *Geol. Jb. R. A* **1990**, 118, 1-111.
76. Gedl, P. Middle Miocene dinoflagellate cysts from the Korytnica clays (Góry Świętokrzyskie Mountains, Poland). *Ann. Soc. Geol. Pol.* **1996**, 66, 191–218.
77. Schreck, M., Matthiessen, J. *Batiacasphaera micropapillata*: palaeobiogeographic distribution and palaeoecological implications of a critical Neogene species complex. *Micropalaeont. Soc. Spec. Publ.* **2013**, 5, 301–314.
78. Gedl, P. Palynofacies of the Miocene deposits in the Gliwice area (Upper Silesia, Poland). *Bull. Pol. Acad. Sci., Earth Sci.* **1997**, 45, 191–201.

79. Rochon, A., de Vernal, A., Turon, J.L., Matthiessen, J., Head, M.J. Distribution of recent dinoflagellate cysts in surface sediments from the North Atlantic Ocean and adjacent seas in relation to sea-surface parameters. *Am. Assoc. Strat. Palynol. Found., Contrib. Ser.* **1999**, 35, 146 pp.
80. Schreck, M., Meheust, M., Stein, R., Matthiessen, J. Response of marine palynomorphs to Neogene climate cooling in the Iceland Sea (ODP Hole 907A). *Mar. Micropaleont.* **2013**, 101, 49–67.
81. Gedl, P. Palaeoenvironmental and sedimentological interpretations of the palynofacies analysis of the Miocene deposits from the Jamnica S-119 borehole (Carpathian Foredeep, Poland). *Geol. Quart.* **1999**, 43, 479–492.
82. Guy-Ohlson, D. Prasinophycean algae. In: *Palynology: Principles and Applications*; Jansonius, J., McGregor, D.C., Eds.; American Association of Stratigraphic Palynologists Foundation, Dallas, Texas, **1996**; Volume 1, pp. 181–189.
83. Gedl, P. Dinoflagellate cysts and palynofacies from the upper Badenian (Middle Miocene) of the Roztocze area at Józefów and Żelebsko (Carpathian Foredeep Basin, Poland): palaeoenvironmental implications. *Ann. Soc. Geol. Pol.* **2016**, 86, 273–289.
84. Bradford, M.R., Wall, D.A. The distribution of Recent organic-walled dinoflagellate cysts in the Persian Gulf, Gulf of Oman, and northeastern Arabian Sea. *Palaeontogr., Abt. B* **1984**, 192, 16–84.
85. Gedl, P., Peryt, D. Dinoflagellate cyst, palynofacies and foraminiferal records of environmental changes related to the Late Badenian (Middle Miocene) transgression at Kudryntsi (western Ukraine). *Ann. Soc. Geol. Pol.* **2011**, 81, 331–349.
86. Peryt, D., Gedl, P., Peryt, T.M. Foraminiferal and palynological records of the Late Badenian (Middle Miocene) transgression in Podolia (Shchyrets near Lviv, western Ukraine). *Geol. Quart.* **2014**, 58, 465–484.
87. Gedl, P., Peryt, D., Peryt, T.M. Foraminiferal and palynological organic matter records of the Upper Badenian (Middle Miocene) deposits at Anadoly (marginal part of the Ukrainian Carpathian Foredeep Basin). *Geol. Quart.* **2016**, 60, 517–536.
88. Head, M.J. Neogene occurrences of the marine acritarch genus *Nannobarbophora* Habib and Knapp, 1982 emend., and the new species *N. gedlii*. *Jour. Paleont.* **2003**, 77, 382–385.
89. Gedl, P. In situ and recycled dinoflagellate cysts from Middle Miocene deposits at Bęczyn, Carpathian Foredeep, Poland. *Studia Geol. Pol.* **2005**, 124, 371–394.
90. Jiménez-Moreno, G., Head, M.J., Harzhauser, M. Early and Middle Miocene dinoflagellate cyst stratigraphy of the Central Paratethys, Central Europe. *Jour. Micropaleont.* **2006**, 25, 113–139.
91. Oszaśt, J. The Miocene vegetation of a sulphur bed at Piaseczno near Tarnobrzeg (Southern Poland) (in Polish with English summary). *Acta Palaeobot.* **1967**, 8, 3–29.
92. Sadowska, A. Sarmatian palynoflora from Jamnica near Tarnobrzeg (Carpathian Foredeep) - environmental and climatic implications. *Geol. Quart.* **1999**, 43, 493–498.
93. Schlütz, F., Shumilovskikh, L.S. On the relation of *Potamomyces armatisporus* to the fossil form-type *Mediaverrunites* and its taxonomical and ecological implications. *Fung. Ecol.* **2013**, 6, 309–315.
94. Worobiec, G., Neumann, F.H., Worobiec, E., Nitz, V., Hartkopf-Fröder, C. New fungal cephalothecoid-like fructifications from central European Neogene deposits. *Fung. Biol.* **2017**, 121, 285–292.
95. Worobiec, G., Worobiec, E., Gedl, P., Kasiński, J.R., Peryt, D., Widera, M. Terrestrial-aquatic wood-inhabiting ascomycete *Potamomyces* from the Miocene of Poland. *Acta Palaeontol. Pol.* **2022**, 67, 737–744.
96. Hawksworth, D.L., van Geel, B., Wiltshire, P.E. The enigma of the *Diporotheca* palynomorph. *Rev. Palaeobot. Palynol.* **2016**, 235, 94–98.
97. Worobiec, G., Worobiec, E., Gedl, P., Kowalski, R., Peryt, D., Tietz, O. Fossil history of fungus host-specificity: Association of conidia of fossil *Asterosporium asterospermum* with macro- and microremains of *Fagus*. *Fungal Biol.* **2023**, 127, 1312–1320.
98. Worobiec, E., Worobiec, G., Gedl, P. Occurrence of fossil bamboo pollen and a fungal conidium of *Tetraploa* cf. *aristata* in Upper Miocene deposits of Józefina (Poland). *Rev. Palaeobot. Palynol.* **2009**, 157, 211–217.
99. Grabowska, I., Słodkowska, B. *Katalog profili osadów trzeciorzędowych opracowanych palinologicznie* (in Polish). PIG, Warszawa, **1993**; pp. 80.
100. Ważyńska, H. Introduction. *Pr. Państw. Inst. Geol.* **1998**, 160, 5–8.
101. Oszaśt, J. Pollen analysis of Tortonian clays from Stare Gliwice in Upper Silesia, Poland (in Polish with English summary). *Monogr. Botan.* **1960**, 9, 1–47.
102. Dyjor, S., Sadowska, A. Problem of the Badenian-Sarmatian boundary at Stara Kuźnia region near Kędzierzyn (Silesia) in the light of palinological investigations (in Polish with English summary). *Acta Palaeobot.* **1984**, 24, 27–51.
103. Sadowska, A. Former palynological studies of the Tertiary in the western part of Carpathian Foredeep in Poland (in Polish with English summary). *Prz. Geol.* **1996**, 44, 1039–1042.
104. Sadowska, A. Miocene palynology in the Gliwice Region (Upper Silesia), Poland. *Bull. Pol. Acad. Sci., Earth Sci.* **1997**, 45, 203–210.
105. Durska, E. The Badenian Salinity Crisis in the palynological record: vegetation during the evaporative event (Carpathian Foredeep, southern Poland). *Ann. Soc. Geol. Pol.* **2017**, 87, 213–228.

106. Kita, Z. Palynological analysis of Tortonian deposits from the borehole Klaj 1 (East of Kraków) (in Polish with English summary). *Roczn. Polsk. Tow. Geol.* **1963**, *33*, 517–526.
107. Syabryaj, S.V., Stuchlik, L. Palaeofloristic and palaeoclimatic reconstruction on the territories of Ukraine and Poland during the Badenian-Sarmatian. *Acta Palaeobot.* **2004**, *44*, 55–68.
108. Zachos, J., Pagani, M., Sloan, L., Thomas, E., Billups, K. Trends, rhythms, and aberrations in global climate 65 Ma to present. *Science* **2001**, *292*, 686–693.
109. Syabryaj, S.V., Stuchlik, L. Development of flora and vegetation of the Ukrainian Eastern Carpathians and Polish Western Carpathians in the Neogene. *Acta Palaeobot.* **1994**, *34*, 165–194.
110. Kvaček Z., Kováč, M., Kovar-Eder, J., Doláková, N., Jechorek, H., Parashiv, V., Kováčová, M., Sliva, L. Miocene evolution of landscape and vegetation in the Central Paratethys. *Geol. Carpath.* **2006**, *57*, 295–310.
111. Hudáčková, N., Ruman, A., Plašienková, I., Jamrich, M., Halásová, E., Kiss, P., Kováčová, M., Babejová-Kmecová, J., Kováč, M. Badenian/Sarmatian foraminifera shift in the Central Paratethys: two methods comparison – a morphogroup and species approach. In: *Proceedings of the Geologica Carpathica 70 Conference, Smolenice Castle, Slovakia, October 9–11, 2019*; Broska, I., Kohút, M., Tomašových, A., Eds.; **2019**; pp. 144–145.
112. Palcu, D.V., Tulbure, M., Bartol, M., Kouwenhoven, T.J., Krijgsman, W. The Badenian-Sarmatian Extinction Event in the Carpathian foredeep basin of Romania: Paleogeographic changes in the Paratethys domain. *Glob. Planet. Change* **2015**, *133*, 346–358.
113. Nováková, P., Rybár, S., Šarinová, K., Nagy, A., Hudáčková, N., Jamrich, M., Teodoridis, V., Kováčová, M., Šujan, M., Vlček, T., Kováč, M. The late Badenian-Sarmatian (Serravallian) environmental transition calibrated by sequence stratigraphy (eastern Danube Basin, Central Paratethys). *Geol. Carpath.* **2020**, *71*, 291–313.
114. Popov, S.V., Antipov, M.P., Zastrozhnov, A.S., Kurina, E.E., Pinchuk, T.N. Sea-level fluctuations on the northern shelf of the Eastern Paratethys in the Oligocene–Neogene. *Stratigr. Geol. Correl.* **2010**, *18*, 200–224.
115. Simon, D., Palcu, D., Meijer, P., Krijgsman, W. The sensitivity of middle Miocene paleoenvironments to changing marine gateways in Central Europe. *Geology* **2019**, *47*, 35–38.
116. Peryt, D., Gedl, P., Jurek, K., Więclaw, D., Worobiec, E., Worobiec, G., Peryt, T.M. Environmental perturbations around the Badenian/Sarmatian (Middle Miocene) boundary in the Central Paratethys: micropalaeontological and organic geochemical records. *Palaeogeogr., Palaeoclimatol., Palaeoecol.* **2024**. (submitted)
117. Brasier, M.D. The ecology and distribution of Recent foraminifera from the reefs and shoals around Barbuda, West Indies. *Jour. Foram. Res.* **1975**, *5*, 193–210.
118. Piller, W.E. Harzhauser, M. The myth of the brackish Sarmatian Sea. *Terra Nova* **2005**, *17*, 450–455.

**Disclaimer/Publisher's Note:** The statements, opinions and data contained in all publications are solely those of the individual author(s) and contributor(s) and not of MDPI and/or the editor(s). MDPI and/or the editor(s) disclaim responsibility for any injury to people or property resulting from any ideas, methods, instructions or products referred to in the content.